Tracking Seasonal and Monthly Drought with GRACE-based Terrestrial Water Storage Assessments over Major River Basins in South India

K SatishKumar[1], E Venkata Rathnam[2] and Venkataramana Sridhar[3]

[1]Research Scholar, Department of Civil Engineering, National Institute of Technology, Warangal, India

[2]Professor, Department of Civil Engineering, National Institute of Technology, Warangal, India

[3]Deparment of Biological Systems Engineering, Virginia Polytechnic Institute and State University, Blacksburg, VA 24061, USA

[1]satish005@student.nitw.ac.in, [2]evr@nitw.ac.in, [3]vsri@vt.edu (corresponding author)

Abstract

Drought is a complex natural hazard that affects ecosystems and society in several ways and it is important to quantify drought at the river basin scale. Assessment of drought requires both hydrological observations and simulation models as the data are generally scarce. Therefore, we use remote sensing products to help understand drought conditions in four basins in South India. This study analysed the correlation among five drought indices for four seasons: gravity recovery and climate experiment - drought severity index (GRACE-DSI), standardized precipitation index (SPI), self-calibrated palmer drought severity index (sc_PDSI), standardised precipitation-evapotranspiration index (SPEI), and combined climatologic deviation index (CCDI) with GRACE terrestrial water storage anomalies (TWSA) using the Pearson correlation coefficient (r) from 2002 to 2016 over the Godavari, Krishna, Pennar, and Cauvery river basins. Basin scale drought events are evaluated using CCDI, GRACEDSI, sc_PDSI, SPI12, and SPEI12 at seasonal and monthly time scale. Characteristics of drought event analysis are calculated for CCDI monthly. The results showed that GRACE TWS is highly correlated with GRACE-DSI, CCDI, and sc_PDSI. Seasonally, high spatial correlations between CCDI and GRACE-DSI with GRACE TWS are evident for all the river basins. Additionally, correlation is found to exist between sc_PDSI and GRACE TWS as soil moisture content is an operating variable between them. The 12-month SPI and SPEI correlated better with GRACE TWS than the 3 and 6-month periods. Among the four basins, droughts in the Krishna Basin lasted 29 months, longer than in the rest of the basins between 2003 and 2005. Overall, CCDI and GRACE-DSI indices are found to be effective for examining and evaluating the drought conditions at the basin scale.

Keywords: Drought indices, GRACE, Pearson Correlation Coefficient, TWSA, Drought characteristics

1. Introduction

Failed monsoons and increased variability in precipitation trigger drought, having adverse impacts on the ecosystem, agriculture, society, and economy (Mishra and Singh, 2010). In recent decades, with changing climate, drought-related calamities have escalated worldwide (Allen et al., 2011; Kang and Sridhar, 2017a, b; Thilakarathne and Sridhar, 2017). Like many other countries, the frequency of occurrence of droughts increased several fold in India since 1965 (Shewale and Kumar, 2005; Bisht et al., 2017; Setti et al., 2020). The average drought length and severity in India will continue to increase in the future (2010–2099) compared to

the historic period (1979–2005), which leads to serious regional drought problems (Bisht et al., 2019). Drought depends mainly on seasonal variations in precipitation resulting in the occurrence of extreme events (Van Loon and Van Lanen, 2013; Bisht et al., 2018). The drought conditions are further compounded with increasing water demand due to population growth, irrigated agriculture, and industrialisation. The geographical area of India is approximately 3.28 million km^2, of which around 1.07 million km^2 are exposed to various types of drought conditions (Mishra et al., 2009). Increased demand for water leads to overexploitation of surface and subsurface water resources, resulting in conflicts among water users during drought periods. Drought monitoring at the river basin level is therefore necessary for proper evaluation of water resources, management, and mitigation strategies.

Drought is a recurrent feature of climate occurring in all climatic regimes. Precipitation, timing, intensity, duration, temperature, humidity, and wind speed play significant roles in the occurrence of droughts and its effects accumulate gradually over a significant period of several months to years. Subsequently, drought management plans have uncertainties as it is difficult to accurately assess the start and end time, known as a creeping phenomenon. Drought indices are suitable tools for monitoring, quantifying, and evaluating drought, its social and ecological impacts and become predominant in drought characterisation as they reduce the complexity of the drought phenomenon to a single numerical value. Drought indicators have become key and decisive features over time for drought monitoring and early warning systems (Vicente-Serrano et al., 2011). Despite numerous drought indices available to date, there is considerable debate on the effectiveness and applicability of each drought index (Sehgal et al., 2017).

Over the last few decades, PDSI, SPI, and SPEI have been the most extensively used drought indices worldwide (Hayes et al., 2011). Despite their suitability for a variety of water-related sectors, these indices have their limitations. For instance, SPI is extensively related to precipitation, which does not take into account other important variables that bias the characterisation of drought. Similarly, PDSI is calculated using duration and weighting factors derived from the dataset observed over USA regions and therefore limits its implementation to other climate zones (Palmer 1965; Zhang et al., 2018). PDSI also lacks multi-timescale features compared to SPI, making it difficult to compare with runoff and reservoir storage. Wells et al. (2004) proposed a new drought index called self-calibrated PDSI (sc_PDSI), which can be applied to any region considering the local variations. The standardized precipitation evapotranspiration index (SPEI) outperformed SPI and PDSI in evaluating drought characteristics (Vicente-Serrano et al., 2010). Some studies by Mishra and Singh (2010), Dai

(2011a), Zhang et al. (2015), and Kang and Sridhar (2019) examined the competency and shortcomings of these three indices (SPI, SPEI, and PDSI) in depth.

While most of the above-mentioned indices are based on land surface conditions or model simulations, a few are related to remote sensing techniques. At present, remote sensing capabilities have increased several fold, capturing the spatial and temporal variations in land surface fluxes at larger scales than before. Hydrological, meteorological, and agricultural droughts are therefore monitored using remote sensing products. GRACE-related terrestrial water storage (TWS) (Girotto et al., 2017; Zhao et al., 2017a, b) has been recently applied in monitoring and characterising regional droughts and water availability conditions. Cao et al. (2015) introduced the total storage deficit index (TSDI) from GRACE-based change in TWS over Northwest China. Yi and Wen (2016) developed the GRACE-based hydrological drought index (GHDI). For the quantification of drought, Sinha et al. (2017) developed the water storage deficit index (WSDI). Zhao et al. (2017b) developed a new global gridded drought severity index (DSI) from GRACE TWS changes called GRACE-DSI. Sinha et al. (2019) proposed the combined climatologic deviation index (CCDI) utilizing GRACE TWS and precipitation over Indian river basins.

Sinha et al. (2017) characterised drought in India by developing WSDI with GRACE TWS deficits and compared WSDI with SPI, SPEI, and PDSI. Sinha et al. (2019) developed the CCDI, which reports precipitation and TWS variations in combination compared to commonly used drought indices such as SPI, SPEI, PDSI, and GRACE-DSI over major Indian river basins. CCDI appropriately manifests its ability to identify and track droughts at a large scale. It is also provided by low precipitation and high temperature conditions observed in all the basins, which further supports identifying drought events hydro-meteorologically (Sinha et al., 2017). However, understanding of correlation between GRACE TWS and other drought indices is useful to validate and illustrate the relevance of these indices to forecast drought in certain areas (Yang et al., 2020; Zhao et al., 2017b).

From the previous studies, spatial and temporal evaluations of drought were identified using hydrological drought with GRACE TWSA and these studies reported that longer duration and higher severity of drought causes long recovery time (Goncalves et al., 2020; Chen et al., 2019; Zhang et al., 2019). Effect of teleconnection factors on GRACE ground water drought indices were examined and stated that ENSO showed strongest impact on GGDI (Wang et al., 2020). WaterGap Global Hydrology Model was used for calibrating surface and ground water storage

which helped in understanding realistic condition of basin during droughts (Schumacher et al., 2018). Variations of insitu groundwater observations were analysed with GRACE TWSA (Goncalves et al., 2020, and Chen et al., 2019). GRACE-DSI was proposed and analysed with SPI and PDSI to find the variations of intrinsic differences in drought indicators (Liu et al., 2020). Our study extends from the previous studies in performing seasonal correlation analysis between drought indices (SPI12, SPEI12, sc_PDSI, GRACE-DSI and CCDI) and GRACE TWSA over major Indian river basins as there is a gap in our understanding on the suitability of basin-specific indices. In addition, seasonal and monthly drought events were evaluated as generally they are difficult to quantify in terms of the onset and termination of drought, and all the considered drought indices were examined to identify the drought characteristics for each river basin studied here.

Sinha et al. (2019) performed TWSA analysis for four basins in India. The distinguishing features of our study included the assessment of spatial correlation on a seasonal scale between GRACE TWSA and other indices (SPI, SPEI, sc_PDSI, GRACE-DSI and CCDI). This is considered important in identifying the spatial extent of drought-hit areas as the relationship between drought indices and GRACE TWSA has some physical significance. These insights are important as seasonal correlations analysis between drought indices and GRACE TWSA can be useful to examine the applicability of certain drought indices for individual river basins. It should be noted that accurate quantification of beginning and end of drought period is difficult, however, a drought event captured by a drought index offers the signal of both past and future drought. As each drought index is different by construct and variables involved, differences in characterizing drought events are expected among the indices. Therefore, by analyzing several indices as performed in this study, seasonal and monthly drought events offered additional insights into identifying suitable ones from among the indices including SPI12, SPEI12, CCDI, GRACE-DSI, and sc_PDSI. Finally, our study considered Godavari and Krishna river basins similar to Sinha et al (2019), however, additionally Cauvery and Pennar river basins were considered. The four basins considered for this study are driven by monsoon rainfall where 75% of the annual rainfall generally occurs during the monsoon period. It is to provide a comparative assessment of the basins that are subjected to similar climatic and hydrologic conditions. As the Ganges river basin flows are also driven by Himalayan glacier melt. Focusing on the basins shown in our study having a common hydroclimatic characteristic could inform the impact of TWSA in relation to several drought indices.

Spatial correlation analysis is useful in identifying the drought areas that are strongly affected with TWS by considering the relationship between drought indices and GRACE TWSA. As the influence of TWSA with drought indices is spatially unrevealed. With the above perspective, significant seasonal correlations analysis between drought indices and GRACE TWSA could be considered as a standard to examine the applicability of certain drought indices for individual river basins. Therefore, utilizing the existing indices to identify the right index in these basins where hydro-meteorological datasets are scarce is expected to offer insights in assessing future droughts using remote sensing data.

In a country like India, nearly 50% of the people depend on agriculture that relies on the availability of water resources from the regions' water bodies and impoundments. However, there is lack of data on water storage in several regions of the country. Along with water storage availability, soil moisture data form another missing dataset required to understand the water budget. Remote sensing-based assessments can alleviate the data deficiencies in these basins. However, identifying the right index to quantify storage or drought becomes a problem when we do not know what a suitable index is to consider in these basins. In this study, the overall goal was to characterise the relationship between GRACE TWS and various drought indices in the four river basins between 2002 and 2016 to offer insights into assessing future droughts using remote sensing data. The objectives of the present study are (1) to quantify the drought indices: SPI, SPEI, sc_PDSI, GRACE-DSI, and CCDI using precipitation, temperature, and GRACE TWS datasets, (2) to analyse the correlation between six drought indices and GRACE TWSA using statistical techniques, (3) to determine suitable drought indices based on correlation analysis, and (4) apply drought indices to detect seasonal drought patterns impacted by the changes in TWSA over a decade between 2002 and 2016.

The remaining manuscript is structured as: Section 2 introduces the case study and the data used in the study. Next, the selected indices are described in the methods. Section 3 presents the results of seasonal and monthly correlation analysis as well as drought characterization. Section 4 presents discussions and section 5 summarizes the conclusions.

2. Material and methods

2.1 Study area

India is the seventh largest country in the world comprising 22 major river basins (India- WRIS, 2012) of which four river basins are selected for the study. The Godavari Basin is located in the Deccan Plateau and has a tropical climate with annual precipitation from 755 mm to 1531

mm and annual maximum temperature from 31° C to 34° C. A major part of the basin is covered by agricultural land (59.57%) followed by forest area (29.78%) and water bodies (2.06%) as per the 2005–06 land use/land cover (LULC) (www.india-wris.nrsc.gov.in). The Krishna Basin falls in the Deccan Plateau and Western Ghats and its annual precipitation and mean temperature are 859 mm and 26 °C, respectively. Approximately 76% of the basin is covered by agricultural areas and 10% by forests. The Cauvery Basin falls in three agro-climatic zones with tropical and sub-tropical climates. The mean annual precipitation is 1075 mm and mean monthly temperature varies from 23 °C to 28 °C. The basin is dominated by agricultural lands with 66% followed by forest areas with 21%. The Pennar Basin falls in two agro-climate zones with mean annual precipitation of 770 mm, and mean minimum and maximum temperature of 21 °C and 32 °C. From the LULC assessment of 2005–06, 59%, 20%, and 5% of the basin were covered with agricultural lands, forests, and water bodies, respectively. Additional details of these river basins are shown in Table 1 and Figure 1.

Several studies have shown consistencies in the quantitative analyses using the GRACE-based TWS estimates over large areas. However, spatial resolution of GRACE data limited its application over small areas and the results were also not satisfactory (Seo et al., 2009). Therefore, we take an approach to intercompare several indices and validate the findings from the earlier studies. Additionally, in India, GRACE related studies are limited to either large river basins (Ganges, Indus, Bramhaputra, Mahanadi, Godavari, and Krishna) or large homogeneous rainfall zones. Furthermore, rivers chosen for this study are mostly dependent on the southwest monsoon and they constitute the rice bowls of South India where 48% of the population depends on agriculture out of more than 200 million population. We believe studies such as this will add value and insights into managing water resources in this critical region.

2.2 Data

2.2.1 Meteorological data

In the present study, precipitation and temperature gridded data from the India Meteorological Department (IMD) are considered for 1975–2016 with a spatial resolution of 1° × 1° and monthly temporal resolution for the study area. (Rajeevan et al., 2008; Srivastava et al., 2009).

2.2.2 Terrestrial Water Storage Anomaly (TWSA) from GRACE

In this study, the latest release of GRACE monthly mass grids (RL 06) processed at Jet Propulsion Laboratory (JPL) RL06M.MSCNv02 (https://grace.jpl.nasa.gov) are used for analysis. The GRACE data are considered from 2002–2016. The JPL RL06 surface mass data

form a unique framework, which estimates monthly gravity fields at 3 × 3 degree equal-area spherical cap mass concentration using a priori constraints that minimise the impact of measurement errors (Wiese et al., 2016). Correction of the glacial isostatic adjustment (GIA) has been applied. GRACE JPL mascon data does not need a smoothing filter, as the spherical cap mascon performs as a smoothing function by decreasing the signal strength at spatial scales below 3°. Lost signals are restored by applying gridded scaling factors. Despite its effectiveness, there are long-term limitations for scaling factors in the application of groundwater variations (Landerer and Swenson, 2012). Dataset leakage errors are effectively reduced by the use of scaling factors and CRI filters. Residual errors interpret GRACE measurement errors in addition to lost inter-annual signals.

2.2.3 Self-Calibrated Palmer Drought Severity Index

The Sc_PDSI dataset is collected from the CRU TS website at a spatial resolution of 0.5° × 0.5°. New updated versions are available each year, and CRU TS 4.03 is the current update (http://www.cru.uea.ac.uk/data).

2.3 Method

2.3.1 Processing and analysis of data

In the present study, drought indices are evaluated using gridded precipitation and temperature. GRACE is also increasingly used in water availability assessments (Sridhar et al., 2019) and we employed a similar approach in this study. The missing monthly GRACE datasets are filled by the linear interpolation method and missing values are filled using the mean values calculated in the months before and after a missing month (Sun et al., 2018). Precipitation and temperature gridded data are used for the calculation of SPI and SPEI. The indices SPI and SPEI are evaluated using R (package: SPEI; version 3.5.1; https://www.r-project.org/) for the 3, 6, and 12-month timescale. For the calculation of CCDI and GRACE-DSI, GRACE monthly mass grids (RL 06) are used. The potential impact of short reference period (2002-2016) and long reference period (1975-2016) were evaluated over TWSA (Cammalleri et al., 2019). From the analysis, major variations were not observed in between short and long reference period. For this study the base line period is considered from January 2004 to December 2009 i.e., short reference period. Furthermore, our evaluation of different 5-year periods to consider the reference period showed no significant differences. Positive TWS indicates more water and negative value indicates less water than in the past. The sc_PDSI dataset is directly used for the analysis. Here, all the considered dataset variables are resampled and clipped to the same

spatial extent and resolution as that of GRACE TWS i.e., $1° \times 1°$ using the MATLAB tool. The study area (four basins combined; Figure 1) is covered by 92 cells with a spatial resolution of $1° \times 1°$. Timescales of 3, 6-, and 12-months consider the impact of drought on availability of different water resources.

This study analyses the correlation of drought indices such as SPI, SPEI, sc_PDSI, GRACE DSI, and CCDI with the GRACE TWS dataset. The correlation analysis is performed for four seasons: post-monsoon rabi (January to March), pre-monsoon (April to June), monsoon (July to September), and post-monsoon kharif (October to December). The indices SPI and SPEI are evaluated for 3, 6, and 12-month timescales. GRACE-DSI and CCDI are calculated by following the procedures of Zhao et al. (2017a) and Sinha et al. (2019). The Pearson's correlation analysis is performed for 92 grids between each drought index and the GRACE TWS dataset to obtain the correlation coefficients.

$$r = \frac{\sum_{i=1}^{n}(x_i-\bar{x})(y_i-\bar{y})}{\sqrt{\sum_{i=1}^{n}(x_i-\bar{x})^2 \sum_{i=1}^{n}(y_i-\bar{y})^2}} \quad (1)$$

where r = Pearson's correlation coefficient; $\bar{x}, \bar{y}$ are the means of x and y scores; n = the total number of observations; r ranges between -1 and +1, the highest r (positive or negative) represents the higher correlation between x and y; x represents the GRACE TWS dataset; and y represents the drought index. i is $1,2 \ldots . n$.

Then t-test is evaluated to determine the significant difference between the means of two datasets (e.g., GRACE TWS and SPI) and is calculated for their corresponding 'p' values at the 95% confidence level. The significance is indicated when $p < 0.05$. Spatial maps are prepared using ArcGIS 10.3 for the correlation coefficients along with 'p' values.

The drought categories for SPI are considered from McKee et al. (1993), presented in Table 2(a) and for GRACE-DSI and CCDI are considered from the United States Drought Monitor (USDM) that are classified into D0, D1, D2, D3, and D4 categories (Svoboda et al., 2002; Zhao et al., (2017a)), represented in Table 2(b). Note that the categories of drought presented in this study depend on the range of drought indices obtained for four river basins.

2.3.2 Processing standardized precipitation index (SPI)

SPI is a dimensionless meteorological drought index derived by fitting the gamma distribution to the monthly precipitation dataset (McKee et al., 1993). SPI is simple to compute and is useful for drought evaluation. Here, SPI is computed over 3, 6, and 12-month timescales with monthly

gridded precipitation data at a spatial resolution of 1° × 1° from 2002 to 2016. Positive SPI indicates a wet condition, while the negative SPI implies a dry condition.

2.3.3 Processing standardised precipitation evapotranspiration index (SPEI)

SPI is based on a single hydrological variable, precipitation, and it does not include other variables such as streamflow or evapotranspiration, which may have a profound impact on drought. To overcome this problem, SPEI was developed (Beguería et al., 2010; Vicente-Serrano et al., 2010) using the monthly precipitation and temperature data that are generally available at multiple time scales. Among the three methods available for the calculation of potential evapotranspiration (Thornthwaite, Hargreaves, and Penman–Monteith), the Thornthwaite equation could lead to errors in energy-limited regions (Hobbins et al., 2008), as the Thornthwaite PE is based only on temperature, latitude, and month. The Penman–Monteith equation accounts for the effects of radiation, humidity, and wind speed. However, based on practical considerations the data are unavailable. Therefore, SPEI was estimated using the Hargreaves method to estimate evapotranspiration at three different monthly timescales (3, 6, and 12) using the IMD precipitation and temperature data available at the spatial resolution of 1° × 1° from 2002 to 2016. Positive SPEI indicates a wet condition and negative SPEI indicates a dry condition. Drought characteristics are well assessed with SPEI, as the index is consistent and flexible in terms of space and time in reproducing water deficiencies at different timescales.

2.3.4 Processing self-calibrated palmer drought severity index (sc_PDSI)

Palmer (1965) developed an index called PDSI to assess moisture demand and supply on the basis of a two-layer soil water balance model. Wells et al. (2004), within the framework of PDSI, proposed a self-calibrated PDSI (sc_PDSI) model that automatically adjusts the climatic characteristics (K) and the duration factors evaluated from historical climate data for a particular location. The sc_PDSI is calculated from the precipitation and temperature time series with fixed parameters of soil/surface characteristics at each location. This study considered the global gridded monthly sc_PDSI (0.5° × 0.5°) values from 2002 to 2016.

2.3.5 Processing the GRACE drought severity index

GRACE-DSI is a satellite-based drought index derived from the variations in GRACE TWS. GRACE-DSI provides comparison of drought characteristic across regions and time intervals, without considering any impact of uncertainties related to soil water balance models or the influence of meteorological data. It also integrates the variations in water storage due to human

interventions including withdrawal of groundwater. In this study, GRACE JPL RL06 land water storage data are used for the evaluation of GRACE-DSI following the procedure developed by Zhao et al. (2017a).

GRACE-DSI is calculated as

$$GRACE - DSI_{u,v} = \frac{TWS_{u,v} - \overline{TWS}_v}{\sigma_v} \quad (2)$$

where u is the year from 2002–2016; v is the month ranging from January to December; and $\overline{TWS}_v$ and σ_v are mean and standard deviation of monthly anomalies, respectively. GRACE-DSI is dimensionless quantity.

2.3.6 Processing combined climatologic deviation index (CCDI)

CCDI integrates meteorological, hydrological, and agricultural drought occurrences by incorporating precipitation and TWS anomalies for drought assessment. Thus, the CCDI accounts for variations in surface and subsurface water storages. In this study, IMD gridded precipitation data ($1° \times 1°$) and TWS anomalies from JPL RL06 ($1° \times 1°$) are used in calculating CCDI from 2002–2016 for the four river basins following the procedure proposed by Sinha et al. (2019).

Precipitation anomalies are calculated as

$$PA_x = P_x - P_\mu \quad (3)$$

Here, PA_x is precipitation anomaly, P_x represents monthly deviations of precipitation, and P_μ represents the mean of monthly deviations.

$$PA_y^{clim} = \frac{\sum_{y=1}^{12} PA_{x,y}}{N} \quad (4)$$

$$TSWA_y^{clim} = \frac{\sum_{y=1}^{12} TWSA_{x,y}}{N} \quad (5)$$

$$PA_x^{res} = PA_x - PA_{x,y}^{clim} \quad (6)$$

$$TWSA_x^{res} = TWSA_x - TWSA_{x,y}^{clim} \quad (7)$$

$$CD_x = PA_x^{res} + TWSA_x^{res} \quad (8)$$

$$CCDI_x = \frac{CD_x - CD_\mu}{CD_\sigma} \quad (9)$$

where subscript 'x' denotes the month from 1 to x; 'y' denotes each month of the calendar from 1 to 12; N is the total count of the considered month; '$clim$' and 'res' denote time series of climatology and residuals, respectively; and $'\mu'$ and $'\sigma'$ are the mean and standard deviation.

Severity and duration are calculated as

$$S(t) = M(t) \times T(t) \tag{10}$$

where $S(t)$ is drought event acuteness, $M(t)$ is deficit mean, $T(t)$ is event duration, and t refers to the occurrence of a specific drought event.

3 Results

The potential impact of short reference period (2002-2016) and long reference period (1975-2016) were evaluated over TWSA. For instance, we calculated correlation of SPI 3, 6, and 12 with TWSA for both short (S-SPI3, S-SPI6 and S-SPI12) and long (L-SPI3, L-SPI6 and L-SPI12) reference periods. The results of these correlation analysis are mentioned in the Table 3.

From the correlation analysis, for GRB and PCRB, S-SPI 6 and 12 exhibited high correlation compared to L-SPI 6 and 12 whereas, L-SPI 3 showed high correlation compared to S-SPI 3. For KRB and CRB high correlations were observed in S-SPI 3 and 6 whereas, for SPI12 high correlation was observed for long reference period. From the analysis, major variations were not observed in between short and long reference period. For this study short reference period is considered for further analysis which is referred as SPI instead of S-SPI.

3.1 Seasonal analysis

Seasonal correlation analysis was performed for four seasons over four river basins using Pearson's correlation test. The t-test was evaluated to determine the significant difference between the means of two datasets for their corresponding 'p' values at the 95% confidence level for four seasons. The post monsoon kharif and pre-monsoon seasons (Figure 2) exhibited significant correlation for all the four basins considered in this study. In the monsoon season, part of the Cauvery and Pennar basins showed insignificant correlation as they were not normally impacted by monsoon rains whereas the remaining part showed significant correlation. In the post monsoon rabi season, part of the Godavari, Cauvery, and Pennar basins showed insignificant correlation and the remaining part exhibited significant correlation. The correlation analysis as presented in this study offered insights into spatial and temporal variability between the basins.

3.1.1 GRACE_TWSA and SPI (3, 6, and 12 month) correlation from 2002–16

To identify a suitable index for the assessment of storage and drought conditions, a Pearson correlation coefficient analysis was performed for GRACE_TWSA and SPI (3, 6, and 12 month) and the results showed significant correlation in all seasons of KRB as shown in Figure 2 (a), S1(a), and S1(b). The post-monsoon kharif season indicated high positive significant correlation followed by the post-monsoon rabi season for SPI 3, 6, and 12. The pre-monsoon and monsoon seasons showed positive correlation, with a few negative correlations in the upper (Western Ghats) and southern (Tungabhadra River) parts for SPI 3, 6, and 12. CRB showed significant correlation in post-monsoon kharif and pre-monsoon seasons for SPI 3 (Figure S1(a)), 6 (Figure S1(b)), and 12 (Figure 2 (a)) months, and insignificant correlation was observed for the monsoon and post monsoon rabi seasons for SPI 3, 6, and 12. From Figure 2 (a), GRB showed an almost positive significant correlation in the post-monsoon kharif season followed by the pre-monsoon and monsoon seasons with some negative significant correlations. In the post-monsoon rabi season, insignificant positive and negative correlations were observed in the mid to upper portions of GRB for SPI 3, 6, and 12. In case of SPI 3 and 6, GRB showed significant positive correlation for post-monsoon kharif season whereas, for monsoon and premonsoon seasons significant positive and negative correlations were observed. PCRB showed a significant positive correlation for SPI12 whereas, for SPI 3 and 6 significant positive and negative correlation were observed in the pre-monsoon season. In the monsoon season, insignificant positive and negative correlations were observed in the middle and coastlines of PCRB for SPI 3, 6, and 12. The post-monsoon kharif season showed significant positive correlations for SPI 3, 6, and 12. The post-monsoon rabi season showed insignificant correlation in the south and significant correlation for remaining portion of SPI 3, 6, and 12. Figure S1(a) and S1(b) represents the Pearson's correlation between (a) GRACE TWS and SPI3 and (b) GRACE TWS and SPI6.

3.1.2 GRACE_TWSA and SPEI (3, 6, and 12 month) correlation from 2002–16

Similar analysis of correlation between GRACE_TWSA and SPEI 3 (Figure S2 (a)), 6 (Figure S2(b)), and 12 (Figure 2 (b)) months has shown significant positive correlation in the post-monsoon kharif and monsoon seasons and the pre-monsoon season of SPEI 6 and 12 months, whereas few negative correlations were exhibited in SPEI 3 (upper portion and west) as shown in Figure S2 (a). The post-monsoon rabi indicated highly significant positive correlation in SPEI 6 and 12 months, partly positive and negative (middle and downstream) significant

correlation in the SPEI 3. The GRB presented almost significant positive correlation in the post-monsoon kharif (SPEI 3 and 6). The monsoon season of SPEI 3 and 6, and the pre-monsoon season of SPEI 6 exhibited more positive and a few negative significant correlations. The monsoon season of SPEI 12, the pre-monsoon season of SPEI 3 and 12, and the post-monsoon kharif season exhibited partially significant positive and negative correlations. The post-monsoon rabi season indicated significant positive and negative correlations, and insignificant positive and negative correlations in the middle portion for SPEI 6 and 12. PCRB showed positive correlation in the post monsoon kharif and pre-monsoon seasons for SPEI 3, 6, and 12. In the post-monsoon rabi season, insignificant correlations were observed in the south. Similarly, during the monsoon season, insignificant correlations (middle and coast) were observed. In CRB, highly significant positive correlations were observed in almost all the SPEI 3, 6, and 12 months of post-monsoon kharif and pre-monsoon seasons. Insignificant correlations were observed in the monsoon and the post-monsoon rabi season of all SPEI 3, 6, and 12. Figure S2(a) and S2(b) represents the Pearson's correlation between (a) GRACE TWS and SPEI3 and (b) GRACE TWS and SPEI6.

3.1.3 GRACE_TWSA and GRACE_DSI correlation from 2002–16

The analysis of GRACE_TWSA and GRACE_DSI Pearson correlation exhibited highly positive correlation in almost all seasons as shown in Figure 2 (c). KRB exhibited positive significant correlation in all seasons. GRB indicated highly significant positive correlations in the pre-monsoon, post-monsoon kharif, and monsoon seasons; however, insignificant correlations were observed in the middle and upper portions of the post-monsoon rabi season. CRB exhibited significant highly positive correlations in the post-monsoon kharif and pre-monsoon seasons whereas insignificant correlations were observed in the monsoon and post-monsoon rabi seasons. PCRB exhibited a highly significant positive correlation in the pre-monsoon season. Insignificant positive correlations were observed in the post-monsoon rabi (down south) and monsoon seasons (along the coast and middle portion).

3.1.4 GRACE_TWSA and CCDI correlation from 2002–16

The correlation of GRACE_TWSA with CCDI exhibited highly positive correlations for all seasons as shown in Figure 2 (d). KRB demonstrated highly significant positive correlation for all seasons due to anomalies of precipitation and terrestrial water storage. GRB indicated highly significant positive correlation in the pre-monsoon and post-monsoon kharif seasons, followed by the monsoon season. In the post-monsoon rabi season, an insignificant positive correlation

was noted over the upper portions of GRB. CRB exhibited significant highly positive correlations in the post-monsoon kharif followed by the pre-monsoon season. The monsoon season presented insignificant correlations following the post-monsoon rabi season. CCDI demonstrates changes in surface, near surface, and storage in the subsurface layers similar to GRACE TWS.

3.1.5 GRACE_TWSA and sc_PDSI correlation from 2002–16

Similar assessment of correlation for GRACE_TWSA with sc_PDSI showed positive correlation in almost all seasons as shown in Figure 2 (e). KRB exhibited significant positive correlation in the post-monsoon kharif and rabi seasons followed by the pre-monsoon and monsoon seasons. GRB showed significant positive correlation in the post-monsoon kharif followed by pre-monsoon and monsoon seasons. CRB showed highly significant positive correlations in the post-monsoon kharif and pre-monsoon seasons, whereas insignificant correlations were observed in the monsoon and post-monsoon rabi seasons. PCRB presented both significant positive and negative correlation in the pre-monsoon season. The post-monsoon rabi season represented insignificant correlation specifically in the south and significant positive correlation in the north and middle portion of PCRB. The post-monsoon kharif exhibited significant positive correlation.

3.1.6 Basin wide seasonal drought event analysis

Figure 3 represents the seasonal time series of CCDI, GRACE-DSI, sc_PDSI, SPEI12, and SPI12 for the four river basins considered for the study. Here, the solid red, green, orange, yellow and blue lines represent sc_PDSI, SPEI12, GRACE-DSI, and SPI12. For the monsoon season, drought events were observed during 2002–2005, 2009, and 2011. For the post monsoon kharif season, drought events were observed during 2002–2004. In the post monsoon rabi and pre-monsoon seasons, during 2003–2005 a drought event was observed.

Drought event analysis can be explained more elaborately using monthly data of GRACE TWS and other indices. Detailed study of drought event analysis is done using monthly data as explained in further sections.

3.2 Monthly analysis

3.2.1 GRACE_TWSA variations over the river basins

In Figure 4, spatial variations of GRACE TWSA for GRB, KRB, CRB, and PCRB are presented. For GRB, the upper middle portion showed a significant positive TWSA variation,

whereas the upper and lower portions showed positive variations in TWSA. For KRB, the upper portion exhibited highly positive variations of TWSA whereas the middle lower and lower portions exhibited negative variations. For both CRB and PCRB, the lower portions showed positive variations in TWSA whereas the upper portion showed negative variations.

3.2.2 Correlation analysis among commonly used drought indices

The correlation matrix of CCDI, GRACE-DSI, sc_PDSI, SPEI, and SPI drought indices over four basins is shown in Table 4. The correlation matrix of drought indices is evaluated from January 2003 to December 2016. The SPI, and SPEI time series are compared over a 12-month time scale. There was a general agreement across multiple drought indices, despite some differences among the indices considered.

The estimated correlation coefficients r between CCDI and GRACE-DSI for GRB, KRB, CRB, and PCRB are 0.79, 0.8, 0.92, and 0.81. As CCDI and GRACE-DSI are more responsive to GRACE TWS variations, there is a good correlation between CCDI and GRACE-DSI. The highest correlation between these two indices was observed in CRB. GRACE DSI is calculated using a single variable i.e., terrestrial water storage anomaly (Equation 2). Whereas, CCDI is evaluated using the combined effect of precipitation and terrestrial water storage anomalies. Therefore, the difference in correlation is observed between CCDI and GRACE DSI as the precipitation anomaly is included along with terrestrial water storage anomaly. Similarly, scatter plots of CCDI with other indices (sc_PDSI, SPEI12, and SPI12) were also plotted for all basins and represented in Figure 5. As CCDI integrates precipitation and TWS anomalies for drought assessment, SPI12 was evaluated using precipitation, and a good correlation of 0.73, 0.80, 0.74, and 0.75 was observed between CCDI and SPI12 subsequent to GRACE-DSI. Comparatively, CCDI showed a good correlation with SPEI12 and sc_PDSI in the remaining three river basins (KRB, PCRB, and CRB) as shown in Table 4 and Figure 4. GRACE-DSI is highly correlated with CCDI, moderately correlated with SPI12 and SPEI12, and poorly correlated with sc_PDSI.

The sc_PDSI showed high correlation with CCDI and GRACE-DSI compared to other drought indices for KRB, CRB, and PCRB except GRB. Additionally, sc_PDSI displayed good correlation with SPI12 followed by SPEI. Among the four river basins, the lowest correlation coefficient of r = 0.15 was observed between sc_PDSI and SPEI12 for GRB. sc_PDSI was capable at mid-term and long-term time spans whereas SPEI was convenient at a long-term span. SPI12 and SPEI12 were evaluated using precipitation and evapotranspiration and resulted

in good correlation of 0.78, 0.75, 0.71, and 0.74 for GRB, KRB, CRB, and PCRB. SPI12 was well correlated with CCDI (0.80), GRACE-DSI (0.66), sc_PDSI (0.78), and SPEI12 (0.75) for KRB and poorly correlated with other indices for GRB with the lowest being 0.3 between SPI12 and sc_PDSI. SPEI12 was well correlated with the remaining indices for CRB and poorly correlated for GRB. The major part of GRB consists of agricultural lands i.e., 60% and the forest area covers approximately 30%. Demand for surface water exceeds the availability. Therefore, the availability of water storage was less in GRB, which effects the correlation of GRACE TWS with SPI12 and sc_PDSI. Along with the correlation coefficient, the root mean square error (RMSE), mean average error (MAE), and coefficient of determination (R^2) were also calculated for drought indices with CCDI represented in Table 5.

3.2.3 Basin wide drought event analysis

Figure 6 represents the time series of CCDI, GRACE-DSI, sc_PDSI, SPEI12, SPI12, and GRACE TWSA for the four river basins considered in the study. Here, the solid red, green, black, orange, dashed blue, and blue lines represent CCDI, GRACE-DSI, SPI12, sc_PDSI, SPEI12, and GRACE TWSA; the light red shaded area signifies the period of drought events described by the values of these four drought indices given by NRAA, India (NRAA, 2013). For the characterisation, dry spells of three or more months of drought are taken into account in this study (Thomas et al., 2014). Drought events identified by the indices were denoted as 'DE' with the event order and river basin name. For instance, the drought event for the Godavari river was denoted as $DE1^{GRB}$.

In Figure 6 (a), with reference to CCDI, GRACE-DSI, sc_PDSI, SPEI12, SPI12, and GRACE TWSA; four drought events are observed in GRB i.e., during January 2003–August 2003 ($DE1^{GRB}$), April 2004–May 2005 ($DE2^{GRB}$), September 2008–May 2010 ($DE3^{GRB}$), and September 2015–February 2016 ($DE4^{GRB}$). Among the four drought events, $DE1^{GRB}$ and $DE3^{GRB}$ were characterised as D1 (moderate drought), $DE2^{GRB}$ was represented as D2 (severe drought), and $DE4^{GRB}$ as D0 (abnormal drought). $DE3^{GRB}$ was the longest drought period observed in GRB extending for 21 months between 2008 and 2010.

From Figure 6 (b), three drought events are observed for KRB, $DE3^{KRB}$ is characterised as D2 (severe drought) during July 2012–April 2013, $DE1^{KRB}$ and $DE2^{KRB}$ as D1 (moderate drought) during January 2003–May 2005 and June 2012–April 2013, respectively. $DE3^{KRB}$ was the most severe drought identified in the KRB. The longest drought period observed in KRB was $DE1^{KRB}$, which continued for 29 months from 2003 to 2005.

The three drought events identified in CRB with $DE1^{CRB}$ characterised as D3 (extreme drought) from January 2003 to August 2005, which is the longest drought period, are shown in Figure 6(c). $DE2^{CRB}$ and $DE3^{CRB}$ comes under D1 (moderate) and D3 (extreme), respectively. Three drought events are observed for PCRB during January 2003–July 2005 ($DE1^{PCRB}$: characterised as D1), 12 July–13 August ($DE2^{PCRB}$ characterised as D0) and 14 July–15 September ($DE3^{PCRB}$ characterised as D0) as shown in Figure 6 (d). Overall, CCDI and GRACE-DSI were observed as good predictors of drought for the four basins considered in the study.

3.3 Basin scale drought characteristics using CCDI

Table 6 represents the severity and duration characteristics of CCDI for all the basins. In GRB basin, severity was observed as -11.7261 for 22 months of duration (September 2008 to June 2010). A total of 62 months of drought duration was observed in GRB. In KRB, the highest severity (-12.0101) was observed during the 17 months from January 2003 to May 2004. In PCRB, the highest severity (-14.7907) was observed during the 16 months from January 2003 to April 2004. In CRB, the highest severity (-18.8912) during this same period as in KRB. Drought duration of 62 months for GRB, 67 months for KRB, 71 months for PCRB, and 78 months for CRB were observed. Basin scale severity variations are represented in Figure 7.

4 Discussions

This study investigated six different drought indices in four river basins in South India at three different time scales with GRACE TWSA. SPI, a precipitation-based drought index, is linked with various physical processes, topography, atmospheric and oceanic circulation, and local processes in India. Using a single precipitation indicator can be problematic in evaluating the Indian monsoon cycle as moisture, terrain, and vegetation can affect variation in precipitation at the regional and meso scales (Wang et al., 2015). The results suggest that SPI showed almost good significant correlation in the pre-monsoon season and post-monsoon kharif followed by the monsoon and post-monsoon rabi seasons. Significant correlation between GRACE_TWSA and SPI is evident, indicating that GRACE_TWSA can be used in combination with SPI for drought assessment. The agricultural land areas for GRB, KRB, PCRB, and CRB are 59.57%, 75.86%, 58.64%, and 66.21%, respectively (www.india-wris.nrsc.gov.in). Due to different crop patterns in the agricultural land during monsoon and post-monsoon seasons, insignificant correlation is observed between TWS and all other indices.

SPEI indicates the availability of water driven by climate demand similar to that of PDSI, whereas SPI does not include soil moisture. SPEI is the summation of precipitation and

evapotranspiration and measures normalised changes in moisture availability. Evapotranspiration is mainly used to define soil moisture changes and water content in vegetation (Vicente-Serrani et al., 2010). Water levels and moisture conditions are affected by meteorological conditions (physical geography, human interventions) both spatially and temporally (Zhao et al., 2015). A few studies have reported that SPEI is useful to examine variations temporally (Li et al., 2012; Chen et al., 2016). In arid regions, as precipitation and evapotranspiration can be constraints, SPEI produces poor fit results (Beguería et al., 2014). From this study, we conclude that SPEI 3, 6, and 12 months have agreed well with GRACE_TWSA and we concur that GRACE_TWSA can be suitable for drought assessment over large areas.

Correlation between sc_PDSI and GRACE_TWSA showed a better fit. In the calculation of sc_PDSI, soil moisture is considered to be evaluated with evapotranspiration (demand) and precipitation (supply) using the water balance equation. sc_PDSI is considered as a multifactorial water budget indicator that takes into account monthly precipitation, temperature, and soil properties. Soil moisture storage is calibrated by separating the soil column into layers with available moisture at field capacity. The detailed procedure for the evaluation of PDSI and sc_PDSI can be found in Alley (1984), Karl (1986), and Wells et al. (2004). sc_PDSI showed good positive fit for all the seasons except in the monsoon season of PCRB and CRB, and the post-monsoon rabi of GRB, PCRB, and CRB. This result was observed in other studies in which PDSI was constant, while the values of TWS decreased in the summer and spring (Dai et al., 2004; Long et al., 2013). This can be inferred from the fact that variation in the correlation is largely related to the spatial extent of precipitation and more commonly to the atmospheric circulation (Mika et al., 2005). Seasonal fluctuation is observed mainly in large river basins. A high correlation was noted between GRACE_TWSA and sc_PDSI for China (Dai, 2011b). It is clear that the correlation between GRACE_TWSA and sc_PDSI exhibited highly positive correlation compared to all other indices followed by CCDI.

GRACE_DSI is evaluated using GRACE TWS comprising surface and subsurface water components. GRACE-DSI is highly correlated with GRACE_TWSA as it is based on direct measurements of the water balance components that account for water supply (from rainfall) and demand (from evapotranspiration and runoff) (Zhao et al., 2017b). GRACE-DSI and CCDI are also strongly correlated as source for the evaluation of these indices and are the same i.e., as GRACE data.

CCDI is a combined climatologic deviation index with precipitation anomalies and terrestrial water storage. This explains changes in surface, near surface, and groundwater conditions. It is important to understand that the combination of precipitation and storage differences may have triggered disagreements with other indices while it has been proved to be reasonable for good correlation with GRACE_TWSA. It is also observed that CCDI and sc_PDSI correlations are almost identical in all the river basins for all seasons except for Godavari Basin.

The dataset of GRACE_TWSA is a combination of hydroclimatic and anthropogenic factors. Various river basins of varying physical characteristics are considered in this study; therefore, different correlation values with drought indices have been observed. CCDI has performed well compared to all other indices. Subsequently, sc_PDSI, GRACE-DSI, SPEI, and SPI have exhibited good correlation. It is concluded from the results that CCDI and sc_PDSI have performed better to characterise storage and drought.

In this study, the correlation matrix for drought indices (CCDI, GRACE-DSI, sc_PDSI, SPEI12, and SPI12) shown in Table 4 suggested that all the basins had demonstrated high correlation between CCDI and GRACE-DSI, as both are calculated using GRACE TWS dataset comprising all forms of water stored above and below the land surface. SPI12 and SPEI12 are more responsive to precipitation and evapotranspiration, resulting in a high correlation between them. The sc_PDSI showed a better fit for CCDI and GRACE-DSI than other drought indices considered for analysis. This is because sc_PDSI considers the soil moisture content of the model algorithm, which is also the main component in the GRACE-derived TWS. Notwithstanding the inconsistencies between the drought indices and the method used to compute the indices, it is clear that droughts can be better understood by a combination of indices.

5 Conclusions

During the period between 2002 and 2016, we examined and evaluated the drought conditions in four major river basins in India. GRACE-satellite data provide important benefits to the field of hydrology, revealing information about large-scale groundwater depletion, and droughts. CCDI, GRACE-DSI, sc_PDSI, SPEI, and SPI were used to analyse and characterise the stressed regions with GRACE TWSA in four river basins. In addition, multiple drought indices were compared and similarities and differences in drought conditions were investigated. Furthermore, basin scale drought events were evaluated using CCDI, GRACE-DSI, SPEI12,

SPI12, and sc_PDSI. Drought characteristics were evaluated to observe the severity and duration among all the basins using CCDI.

- CCDI and GRACE-DSI correlated well with GRACE TWS in capturing both spatial and temporal drought conditions.
- KRB manifested high storage anomalies leading to strong seasonal fluctuation in drought indices.
- From the drought event analysis of KRB, as it stands out among other basins during 2003 to 2005, the most severe drought lasted for 29 months, while the wettest period was detected during October 2008–October 2011. Assessment of these extreme hydrologic conditions are critical and possible when the analysis is aided with remote-sensing data for better management of regions' the water resources.
- Drought severity and duration were evaluated for CCDI. From a total of 180 months, a period of 62 months for GRB, 67 for KRB, 71 for PCRB, and 78 for CRB were observed. Knowledge about duration and spatial extent of drought from both hindcast and real-time analysis of drought indices within the context of TWS serves as a powerful tool for planning and management of the land and water resources of these major river basins.
- Although differences were found between indices, the shifting trend and peak time were consistent.

This study utilised the existing indices to identify the appropriate index to be considered in these basins and to offer insights in assessing future droughts using remote sensing data. It also provides a basis for real-time monitoring of droughts using GRACE TWS and for the development causative analysis of drought phenomena.

The remote sensing capabilities have improved substantially in capturing the spatial and temporal variations in land surface fluxes over vast areas where ground observations to calculate complex drought indices would be nearly impossible. The study establishes the correlation between TWSA and commonly used drought indices which are proved to be applicable to various basins. Better correlation between GRACE TWSA and other drought indices is useful to validate and illustrate the relevance of these indices to forecast drought in these basins. Their utility to these basins needed a relook and which is what we are providing in this study.

Declaration of Competing Interest

The authors declare that they don't have any conflict of interest.

Funding

This research did not receive any specific grant from funding agencies in the public, commercial, or not-for-profit sectors.

References

Allen, P.M., Harmel, R.D., Dunbar, J.A., Arnold, J.G., 2011. Upland contribution of sediment and runoff during extreme drought: a study of the 1947–1956 drought in the Blackland Prairie, Texas. J. Hydrol. 407, 1–11.

Alley, W.M., 1984. The Palmer drought severity index: limitations and applications. J Clim Appl Meteorol. 23, 1100–1109.

Beguería, S., Vicente-Serrano, S.M., Angulo-Martínez, M., 2010. A multiscalar global drought dataset: the SPEI base: a new gridded product for the analysis of drought variability and impacts. Bull. Am. Meteorol. Soc. 91, 1351–1356.

Beguería, S., Vicente-Serrano, S.M., Reig, F., Latorre, B., 2014. Standardized precipitation evapotranspiration index (SPEI) revisited: parameter fitting, evapotranspiration models, tools, datasets and drought monitoring. Int J Climatol. 34, 3001–3023.

Bisht, D.S., Chatterjee, C., Raghuwanshi, N.S., Sridhar, V., 2017. Spatio-temporal Trends of Rainfall across Indian River Basins. Theor Appl Climatol. 132, 419-436. doi: 10.1007/s00704-017-2095-8.

Bisht, D.S., Chatterjee, C., Raghuwanshi, N.S., Sridhar, V., 2018. An analysis of precipitation climatology over Indian urban agglomeration. Theor Appl Climatol. 133, 421–436. doi:10.1007/s00704-017-2200-z.

Bisht, D.S., Sridhar, V., Mishra, A., Chatterjee, C., Raghuwanshi, N.S., 2019. Drought characterization over India under projected climate scenario. Int J Climatol. 39(4), 1889–1911.

Cammalleri, C., Barbosa, P., Vogt, J.V., 2019. Analysing the Relationship between Multiple-Timescale SPI and GRACE Terrestrial Water Storage in the Framework of Drought Monitoring. Water. 11, 1672.

Cao, Y., Nan, Z., Cheng, G., 2015. GRACE gravity satellite observations of terrestrial water storage changes for drought characterization in the arid land of northwestern China. Remote Sens. 7(1), 1021–1047.

Chen, F., Yang, S.B., Wang, C.L., Wang, R.Y., Wang, H.L., Qi, Y., 2016. Spatial and temporal distribution of spring drought in northwest China based on standardized precipitation evapotranspiration index. J Arid Meteorol. 34, 34–42.

Chen, H., Zhang, W., Nie, N., Guo, Y., 2019. Long-term groundwater storage variations estimated in the Songhua River Basin by using GRACE products, land surface models, and in-situ observations. Sci. Total Environ. 649, 372–387.

Dai, A.G., 2011a. Drought under global warming: a review. Adv Rev. 2, 45–65.

Dai, A.G., 2011b. Characteristics and trends in various forms of the Palmer drought severity index during 1900–2008. J Geophys Res. 116, D12115.

Dai, A.G., Trenberth, K.E., Qian, T.T., 2004. A global data set of Palmer drought severity index for 1870–2002: relationship with soil moisture and effects of surface warming. J Hydrometeorol. 5, 1117–1130.

Girotto, M., De Lannoy, G.J., Reichle, R.H., Rodell, M., Draper, C., Bhanja, S.N., Mukherjee, A., 2017. Benefits and pitfalls of GRACE data assimilation: a case study of terrestrial water storage depletion in India. Geophys. Res. Lett. 44, 4107–4115.

Gonçalves, R.D., Stollberg, R., Weiss, H., Chang, H.K., 2019. Using GRACE to quantify the depletion of terrestrial water storage in Northeastern Brazil: The Urucuia Aquifer System. Sci. Total Environ 135845.

Hayes, M., Svoboda, M., Wall, N., Widhalm, M., 2011. The lincoln declaration on drought indices: universal meteorological drought index recommended. Bull. Am. Meteorol. Soc. 92, 485–488. https://doi.org/10.1175/2010BAMS3103.1.

Hobbins, M.T., Dai, A., Roderick, M.L., Farquhar, G.D., 2008. Revisiting potential evapotranspiration parameterizations as drivers of long-term water balance trends. Geophys. Res. Lett. 35, L12403.

Kang, H., Sridhar, V., 2017a. Combined statistical and spatially distributed hydrological model for evaluating future drought indices in Virginia. J. Hydrol. Reg. Stud. 12, 253-272.

Kang, H., Sridhar, V., 2017b. Assessment of future drought conditions in the Chesapeake Bay watershed. J. Am. Water Resour. Assoc. 54, 160–183. DOI: 10.1111/1752-1688.12600.

Kang, H., Sridhar, V., 2019. Drought assessment with a surface-groundwater coupled model in the Chesapeake Bay watershed. Environ. Model. Softw. 119, 379-389.

Karl, T.R., 1986. The correlation of the palmer drought severity index and Palmer's Z-index to their calibration coefficients including potential evapotranspiration. J Clim Appl Meteorol. 25, 77–86.

Landerer, F.W., Swenson, S.C., 2012. Accuracy of scaled GRACE terrestrial water storage estimates. Water Resour. Res. 48, 1–11. https://doi.org/10.1029/2011WR011453.

Li, W.G., Yi, X., Hou, M.T., Chen, H.L., Chen, Z.L., 2012. Standardized precipitation evapotranspiration index shows drought trends in China. Chin J Eco Agric. 20, 643–649.

Liu, X., Feng, X., Ciais, P., Fu, B., Hu, B., Sun, Z., 2020. GRACE satellite-based drought index indicating increased impact of drought over major basins in China during 2002–2017. Agric For Meteorol. 291, 108057.

Long, D., Scanlon, B., Longuevergne, L., Sun, A., Fernando, D., Save, H., 2013. GRACE satellite monitoring of large depletion in water storage in response to the 2011 drought in Texas. Geophys Res Lett. 40, 3395–3401

Mckee, T.B., Doesken, N.J., Kleist, J., 1993. The relationship of drought frequency and duration to time scales. In: AMS 8th Conf. Appl. Climatol. pp. 179–184 citeulikearticle-id:10490403.

Mika, J., Horvath, S., Makra, L., Dunkel, Z., 2005. The Palmer drought severity index (PDSI) as an indicator of soil moisture. Phys Chem Earth. 30, 223–230.

Mishra, A.K., Singh, V.P., Desai, V.R., 2009. Drought characterization: a probabilistic approach. Stoch. Environ. Res. Risk Assess. 23, 41–55.

Mishra, A.K., Singh, V.P., 2010. A review of drought concepts. J. Hydrol. 391 (1), 202–216.

NRAA., 2013. Contingency and Compensatory Agriculture Plans for Droughts and Floods in India- 2012. Position paper No.6. National Rainfed Area Authority, NASC Complex, DPS Marg, New Delhi-110012, India, 87 p.

Palmer, W.C., 1965. Meteorological Drought. Vol. 30. US Department of Commerce, Weather Bureau, Washington, DC, USA.

Rajeevan, M., Bhate, J., Jaswal, A.K., 2008. Analysis of variability and trends of extreme rainfall events over India using 104 years of gridded daily rainfall data. Geophysical Res. Lttrs. 35, L18707. doi:10.1029/2008GL035143.

Schumacher, M., Forootan, E., van Dijk, A., Schmied, H.M., Crosbie, R., Kusche, J., Döll, P., 2018. Improving drought simulations within the Murray-Darling Basin by combined calibration/assimilation of GRACE data into the WaterGAP Global Hydrology Model. Remote Sens. Environ. 204, 212–228.

Sehgal, V., Sridhar, V., Tyagi, A., 2017. Stratified drought analysis using a stochastic ensemble of simulated and in- situ soil moisture observations, J. Hydrol. 545, 226-250. DOI: 10.1016/j.jhydrol.2016.12.033.

Seo, K.W., Waliser, D.E., Tian, B., Famiglietti, J.S., Syed, T.H., 2009. Evaluation of global land-to-ocean fresh water discharge and evapotranspiration using space-based observations. J. Hydrol. 373, 508–515. https://doi.org/10.1016/j.jhydrol.2009.05.014.

Setti, S., Maheswaran, R., Radha, D., Sridhar, V., Barik, K.K., Narasimham, M.L., 2020. Attribution of hydrologic changes in a tropical river basin to climate and land use change: A case study from India. ASCE J. Hydrol. Eng. 25(8). doi: 10.1061/(ASCE)HE.1943-5584.0001937.

Shewale, M., Kumar, S., 2005. Climatological features of drought incidences in India. Natl. Clim. Centre. Indian Meteorological Department. Govt. of India.

Sinha, D., Syed, T.H., Famiglietti, J.S., Reager, J.T., Thomas, R.C., 2017. Characterizing drought in India using GRACE observations of terrestrial water storage deficit. J. Hydrometeorol. 18 (2), 381–396.

Sinha, D., Syed, T.H., Reager, J.T., 2019. Utilizing combined deviations of precipitation and GRACE-based terrestrial water storage as a metric for drought characterization: A case study over major India river basins. J. Hydrol. 572, 294–307.

Sridhar, V., Ali, S.A., Lakshmi, V., 2019. Assessment and validation of total water storage in the Chesapeake Bay watershed using GRACE. J. Hydrol. Reg. Stud. 24, 100607.

Srivastava, A.K., Rajeevan, M., Kshirsagar, S.R., 2009. Development of High Resolution Daily Gridded Temperature Data Set (1969-2005) for the Indian Region. Atmos. Sci. Let. 10, 249–254. DOI: 10.1002/asl.232.

Sun, Z., Zhu, X., Pan, Y., Zhang, J., Liu, x., 2018. Drought evaluation using the GRACE terrestrial water storage deficit over the Yangtze River Basin, China. Sci. Total Environ. 634, 727-738.

Svoboda, M., LeComte, D., Hayes, M., Heim, R., Gleason, K., Angle, J., Rippey, B., Tinker, R., Palecki, M., Stooksbury, D., Miskus, D., Stephens, S., 2002. The drought monitor. Bull. Am. Meteorol. Soc. 83, 1181–1190.

Thilakarathne, M., Sridhar, V., 2017. Characterization of future drought conditions in the Lower Mekong Basin. Weather. Clim. Extremes. 17, 47-58.

Thomas, A.C., Reager, J.T., Famiglietti, J.S., Rodell, M., 2014. A GRACE-based water storage deficit approach for hydrological drought characterization. Geophys. Res. Lett. 41, 1537–1545. https://doi.org/10.1002/2014GL059323.

Van Loon, A.F., Van Lanen, H.A.J., 2013. Making the distinction between water scarcity and drought using an observation-modeling framework. Water Resour. Res. Vol. 49, 1483-1502. doi:10.1002/wrcr.20147.

Vicente-Serrano, S., Beguería, M.S., López-Moreno, JuanI., 2010. A multiscalar drought index sensitive to global warming: the standardized precipitation evapotranspiration index. J. Clim. 23, 1696–1718. https://doi.org/10.1175/2009JCLI2909.1.

Vicente-Serrano, S., Beguería, M.S., López-Moreno, JuanI., 2011. Comment on "Characteristics and trends in various forms of the Palmer Drought Severity Index (PDSI) during 1900–2008". by Aiguo Dai. J. Geophys. Res. 116, D19112.

Wang, F., Wang, Z., Yang, H., Di, D., Zhao, Y., Liang, Q., 2020. Utilizing GRACE-based groundwater drought index for drought characterization and teleconnection factors analysis in the North China Plain. J. Hydrol. 585, 124849.

Wang, H., Rogers, J.C., Munroe, D.K., 2015. Commonly used drought indices as indicators of soil moisture in China. J. Hydrometeor. 16, 1397–1408. doi:10.1175/JHM-D-14-0076.1.

Wells, N., Goddard, S., Hayes, M.J., 2004. A self-calibrating Palmer Drought Severity Index. J. Clim. 17, 2335–2351.

Wiese, D.N., Landerer, F.W., Watkins, M.M., 2016. Quantifying and reducing leakage errors in the JPL RL05M GRACE mascon solution. Water Resour. Res. 52, 7490–7502.

Yang, P., Zhang, Y., Xia, J., Sun, S. 2020. Identification of drought events in the major basins of Central Asia based on a combined climatological deviation index from GRACE measurements. Atmos. Res. Volume 244, 105105, ISSN 01698095.

Yi, H., Wen, L., 2016. Satellite gravity measurement monitoring terrestrial water storage change and drought in the continental United States. Sci. Rep. 6, 19909.

Zhang, Y., Li, Y., Ge, J., Li, G., Yu, Z., Niu, H., 2018. Correlation analysis between drought indices and terrestrial water storage from 2002 to 2015 in China. Environ Earth Sci. 77, 462. https://doi.org/10.1007/s12665-018-7651-8.

Zhang, D., Liu, X., Bai, P., 2019. Assessment of hydrological drought and its recovery time for eight tributaries of the Yangtze River (China) based on downscaled GRACE data. J. Hydrol. 568, 592–603.

Zhang, B., Zhao, X., Jin, J., Wu, P., 2015. Development and evaluation of a physically based multiscalar drought index: the standardized moisture anomaly index. J Geophys Res. 120, 11575–11588.

Zhao, M., Velicogna, I., Kimball, J.S., 2017a. Satellite observations of regional drought severity in the continental United States using GRACE-based terrestrial water storage changes. J. Clim. 30 (16), 6297–6308.

Zhao, M., Velicogna, I., Kimball, J.S., 2017b. A global gridded dataset of grace drought severity index for 2002–14: Comparison with PDSI and SPEI and a case study of the Australia millennium drought. J. Hydrometeorol. 18 (8), 2117–2129.

Zhao, J., Yan, D.H., Yang, Z.Y., Hu, Y., Weng, B.S., Gong, B.Y., 2015. Improvement and adaptability evaluation of standardized precipitation evapotranspiration index. Acta Phys Sin. 64, 049202. https://doi.org/10.7498/aps.64.04920 2.

Figure Captions

Figure 1 Study region map showing river basins considered for the study. (1. GRB, 2. KRB, 3. PCRB, 4. CRB)

Figure 2 Pearson's correlation between (a) GRACE TWS and SPI12, (b) GRACE TWS and SPEI12, (c) GRACE TWS and GRACE DSI, (d) GRACE TWS and CCDI, and (e) GRACE TWS and sc_PDSI

Figure 3 Seasonal timeseries of GRACE TWSA, CCDI, GRACE DSI, SPEI12, scPDSI, and SPI12 for (a) Godavari, (b) Krishna, (c) Cauvery, and (d) Pennar and East rivers between Pennar and Cauvery river basins. Red bands indicate major drought events.

Figure 4 Spatial variation in GRACE TWSA during July 2003–July 2005 drought event over GRB, KRB, CRB, and PCRB.

Figure 5 Basin wide scatter plots for (a) GRB, (b) KRB, (c) CRB, and (d) PCRB between GRACE TWS and CCDI

Figure 6 Monthly timeseries of GRACE TWSA, CCDI, GRACE DSI, SPEI12, scPDSI, and SPI12 for (a) Godavari, (b) Krishna, (c) Cauvery, and (d) Pennar and East rivers between Pennar and Cauvery river basins. Red bands indicate major drought events.

Figure 7 Drought severity computed for each event identified by CCDI for all four basins. Stem plots (blue lines) stand for the severity of each drought event.

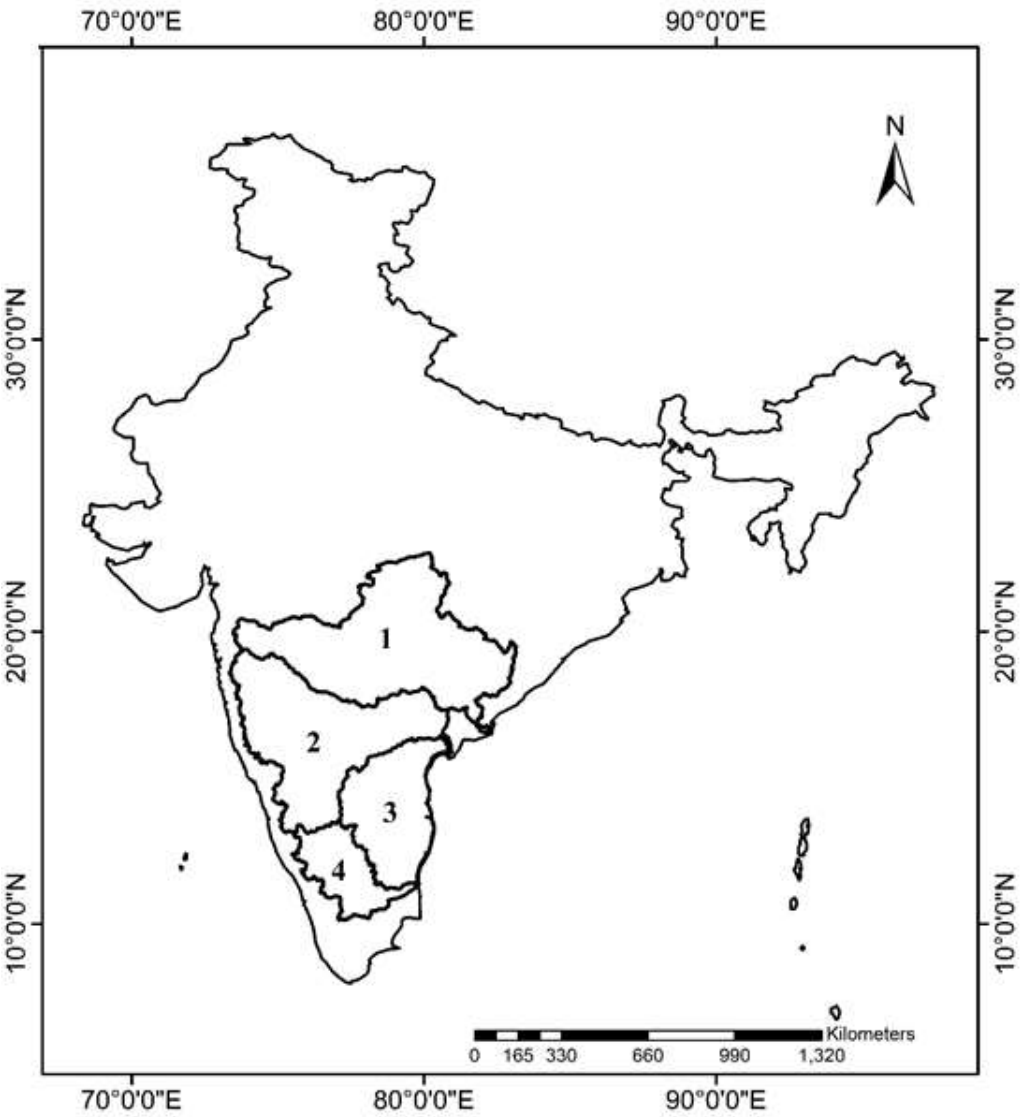
70°0'0"E
80°0'0"E
90°0'0"E
30°0'0"N
20°0'0"N
10°0'0"N
N
1
2
3
4
Kilometers
0 165 330 660 990 1,320

Figure 1

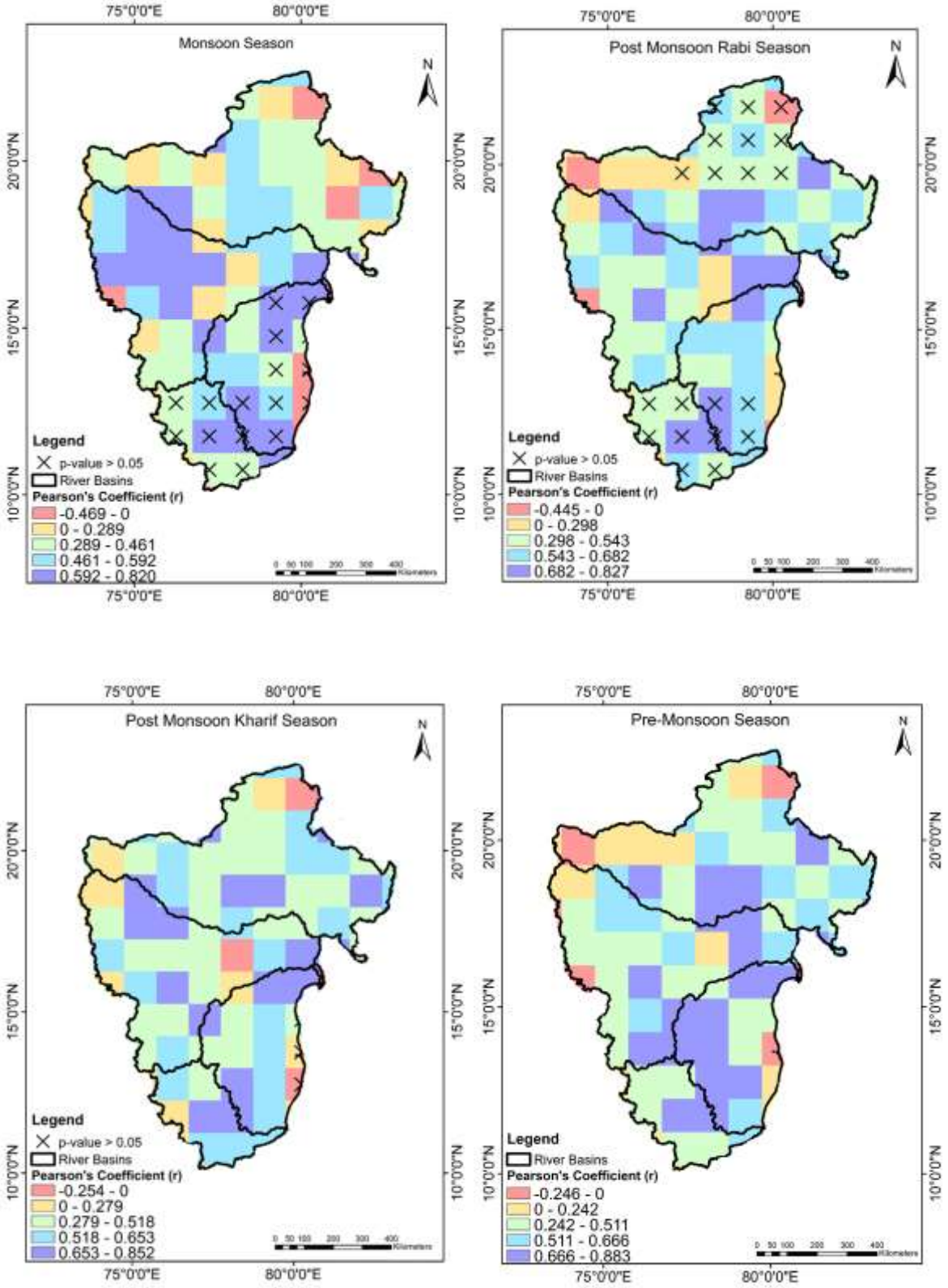
Monsoon Season
Legend
p-value > 0.05
River Basins
Pearson's Coefficient (r)
-0.469 - 0
0 - 0.289
0.289 - 0.461
0.461 - 0.592
0.592 - 0.820
Post Monsoon Rabi Season
Legend
p-value > 0.05
River Basins
Pearson's Coefficient (r)
-0.445 - 0
0 - 0.298
0.298 - 0.543
0.543 - 0.682
0.682 - 0.827
Post Monsoon Kharif Season
Legend
p-value > 0.05
River Basins
Pearson's Coefficient (r)
-0.254 - 0
0 - 0.279
0.279 - 0.518
0.518 - 0.653
0.653 - 0.852
Pre-Monsoon Season
Legend
River Basins
Pearson's Coefficient (r)
-0.246 - 0
0 - 0.242
0.242 - 0.511
0.511 - 0.666
0.666 - 0.883
75°0'0"E
80°0'0"E
20°0'0"N
15°0'0"N
10°0'0"N
N

Figure 2(a)

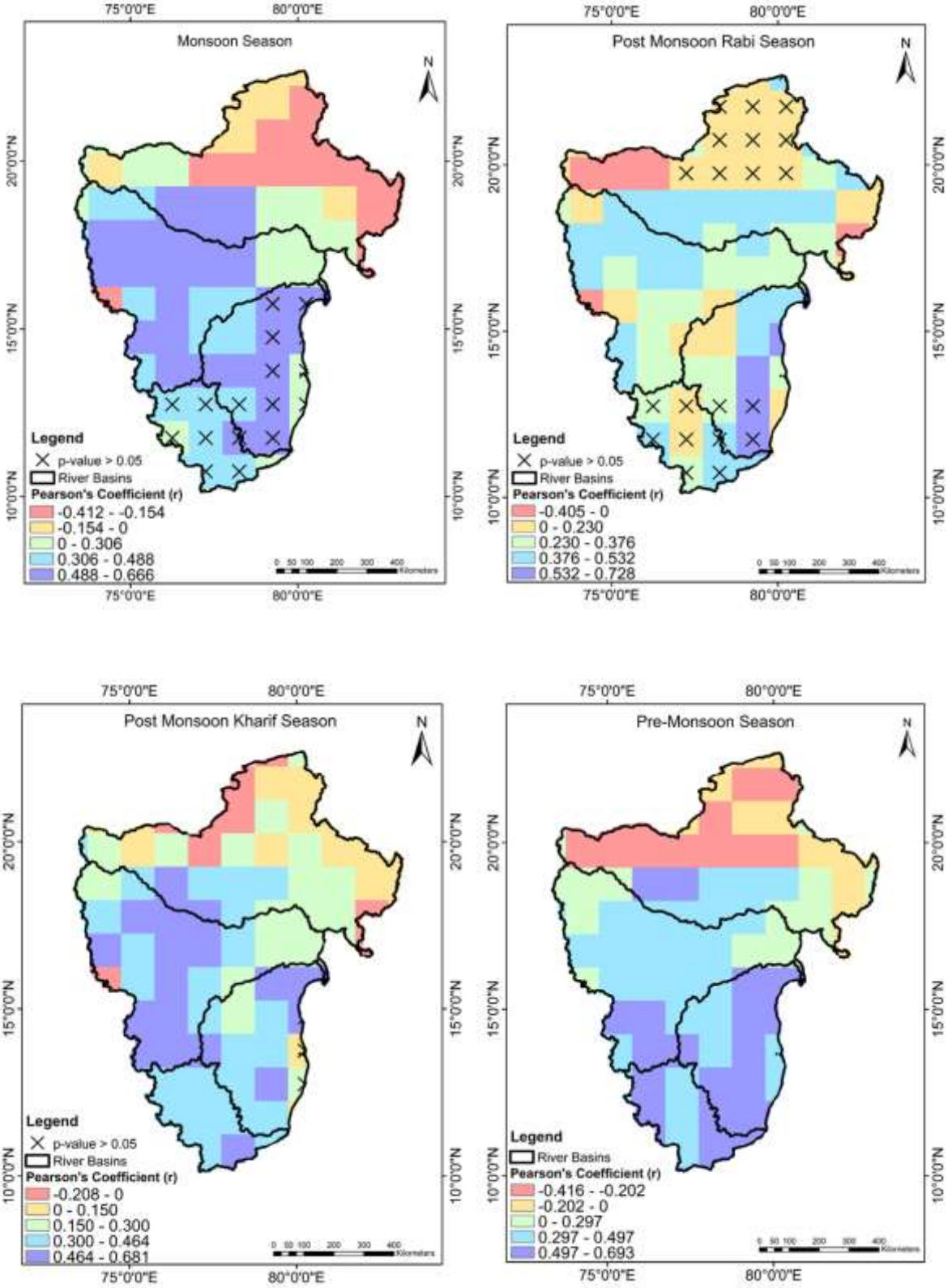
Monsoon Season
Legend
p-value > 0.05
River Basins
Pearson's Coefficient (r)
-0.412 - -0.154
-0.154 - 0
0 - 0.306
0.306 - 0.488
0.488 - 0.666
Post Monsoon Rabi Season
Legend
p-value > 0.05
River Basins
Pearson's Coefficient (r)
-0.405 - 0
0 - 0.230
0.230 - 0.376
0.376 - 0.532
0.532 - 0.728
Post Monsoon Kharif Season
Legend
p-value > 0.05
River Basins
Pearson's Coefficient (r)
-0.208 - 0
0 - 0.150
0.150 - 0.300
0.300 - 0.464
0.464 - 0.681
Pre-Monsoon Season
Legend
River Basins
Pearson's Coefficient (r)
-0.416 - -0.202
-0.202 - 0
0 - 0.297
0.297 - 0.497
0.497 - 0.693
75°0'0"E
80°0'0"E
20°0'0"N
15°0'0"N
10°0'0"N
N

Figure 2(b)

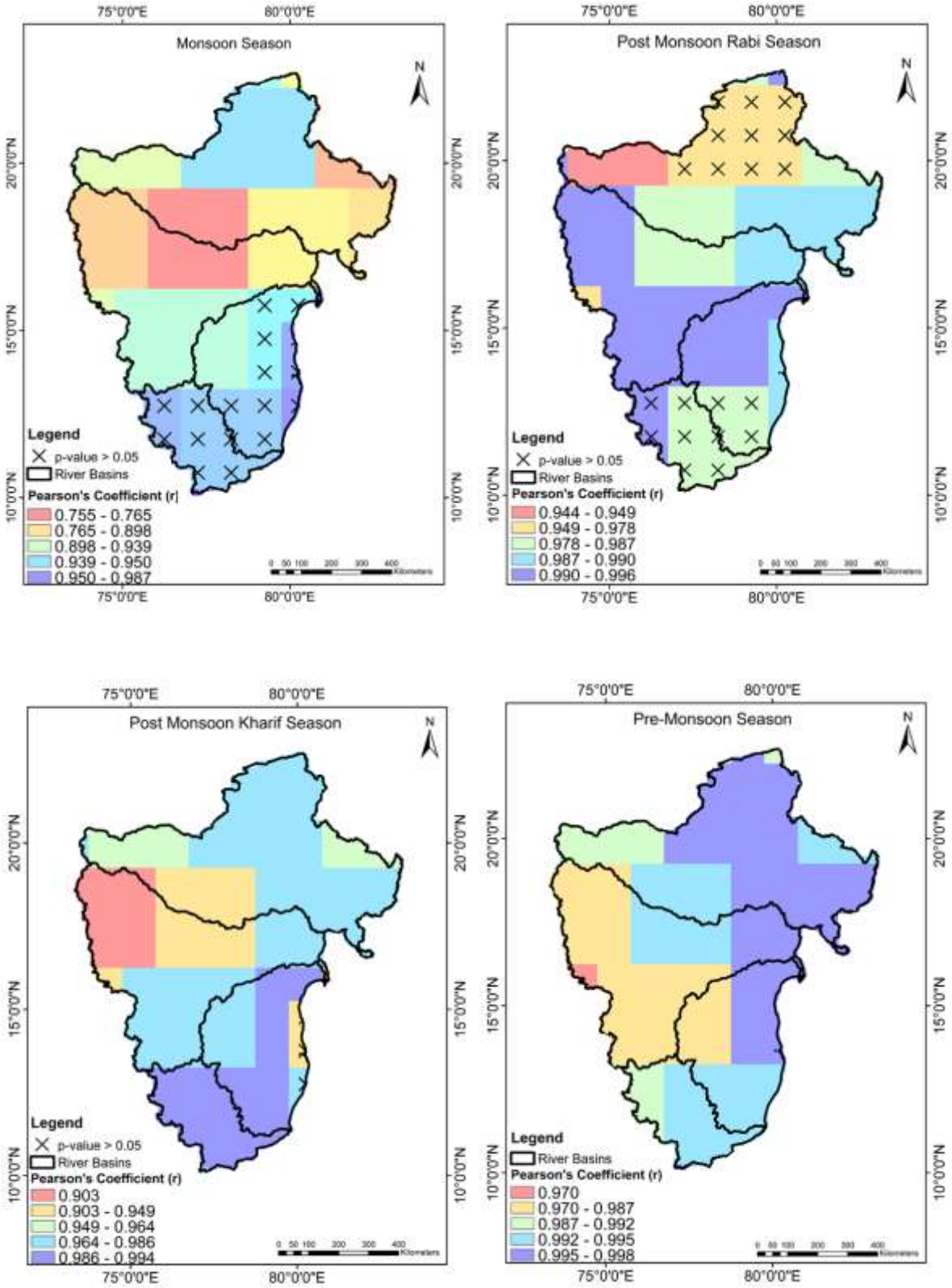
Monsoon Season
Legend
p-value > 0.05
River Basins
Pearson's Coefficient (r)
0.755 - 0.765
0.765 - 0.898
0.898 - 0.939
0.939 - 0.950
0.950 - 0.987
Post Monsoon Rabi Season
Legend
p-value > 0.05
River Basins
Pearson's Coefficient (r)
0.944 - 0.949
0.949 - 0.978
0.978 - 0.987
0.987 - 0.990
0.990 - 0.996
Post Monsoon Kharif Season
Legend
p-value > 0.05
River Basins
Pearson's Coefficient (r)
0.903
0.903 - 0.949
0.949 - 0.964
0.964 - 0.986
0.986 - 0.994
Pre-Monsoon Season
Legend
River Basins
Pearson's Coefficient (r)
0.970
0.970 - 0.987
0.987 - 0.992
0.992 - 0.995
0.995 - 0.998
75°0'0"E
80°0'0"E
20°0'0"N
15°0'0"N
10°0'0"N
N

Figure 2(c)

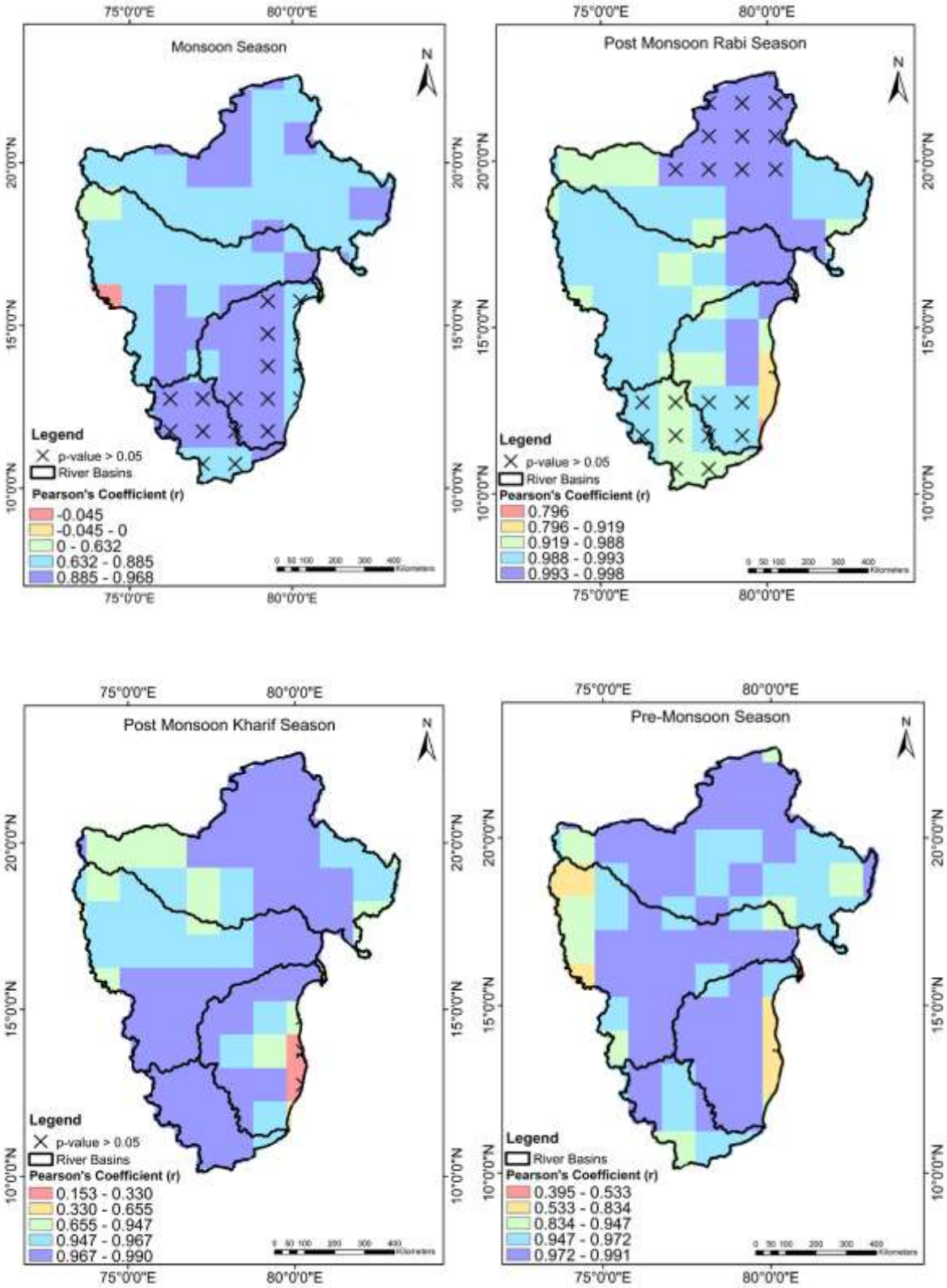
Monsoon Season
Legend
p-value > 0.05
River Basins
Pearson's Coefficient (r)
-0.045
-0.045 - 0
0 - 0.632
0.632 - 0.885
0.885 - 0.968
Post Monsoon Rabi Season
Legend
p-value > 0.05
River Basins
Pearson's Coefficient (r)
0.796
0.796 - 0.919
0.919 - 0.988
0.988 - 0.993
0.993 - 0.998
Post Monsoon Kharif Season
Legend
p-value > 0.05
River Basins
Pearson's Coefficient (r)
0.153 - 0.330
0.330 - 0.655
0.655 - 0.947
0.947 - 0.967
0.967 - 0.990
Pre-Monsoon Season
Legend
River Basins
Pearson's Coefficient (r)
0.395 - 0.533
0.533 - 0.834
0.834 - 0.947
0.947 - 0.972
0.972 - 0.991
75°0'0"E
80°0'0"E
20°0'0"N
15°0'0"N
10°0'0"N
N

Figure 2(d)

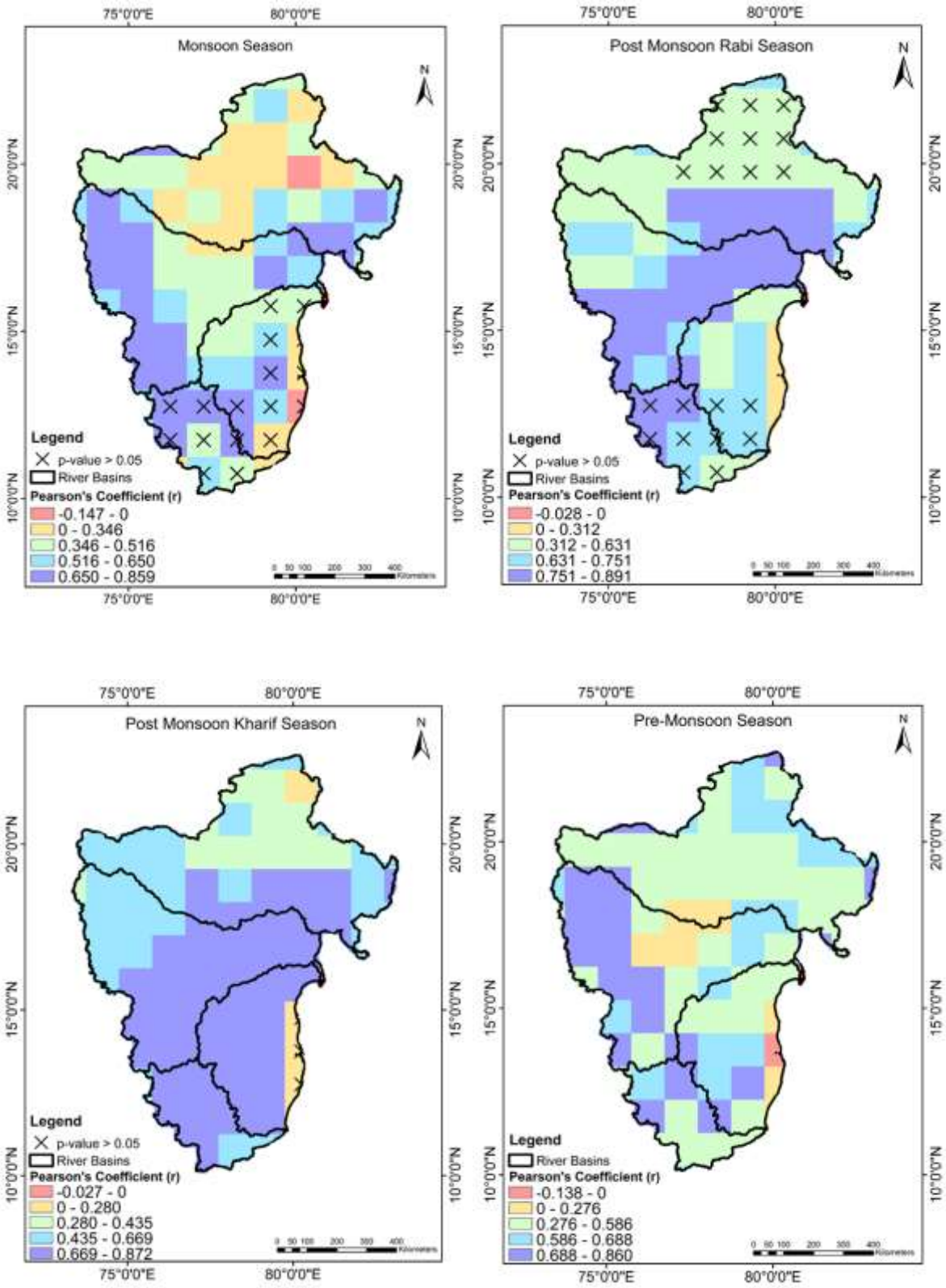
Monsoon Season
Legend
p-value > 0.05
River Basins
Pearson's Coefficient (r)
-0.147 - 0
0 - 0.346
0.346 - 0.516
0.516 - 0.650
0.650 - 0.859
Post Monsoon Rabi Season
Legend
p-value > 0.05
River Basins
Pearson's Coefficient (r)
-0.028 - 0
0 - 0.312
0.312 - 0.631
0.631 - 0.751
0.751 - 0.891
Post Monsoon Kharif Season
Legend
p-value > 0.05
River Basins
Pearson's Coefficient (r)
-0.027 - 0
0 - 0.280
0.280 - 0.435
0.435 - 0.669
0.669 - 0.872
Pre-Monsoon Season
Legend
River Basins
Pearson's Coefficient (r)
-0.138 - 0
0 - 0.276
0.276 - 0.586
0.586 - 0.688
0.688 - 0.860
75°0'0"E
80°0'0"E
20°0'0"N
15°0'0"N
10°0'0"N
N

Figure 2(e)

(a) Monsoon season

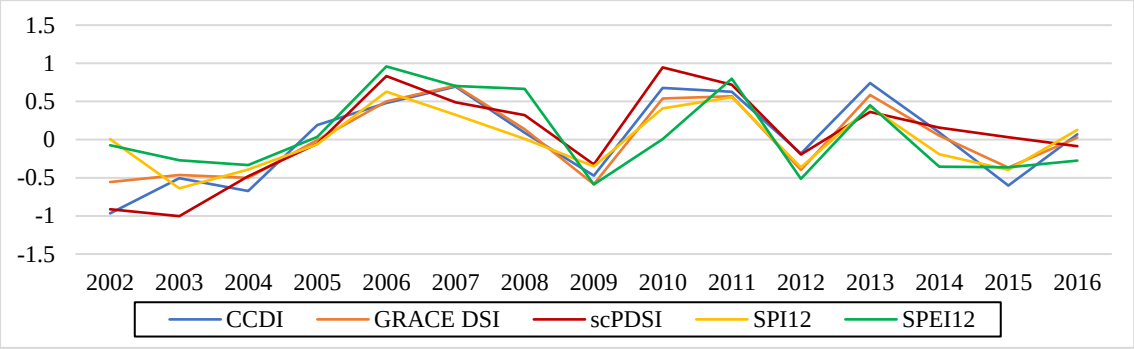

(b) Post Monsoon Kharif season

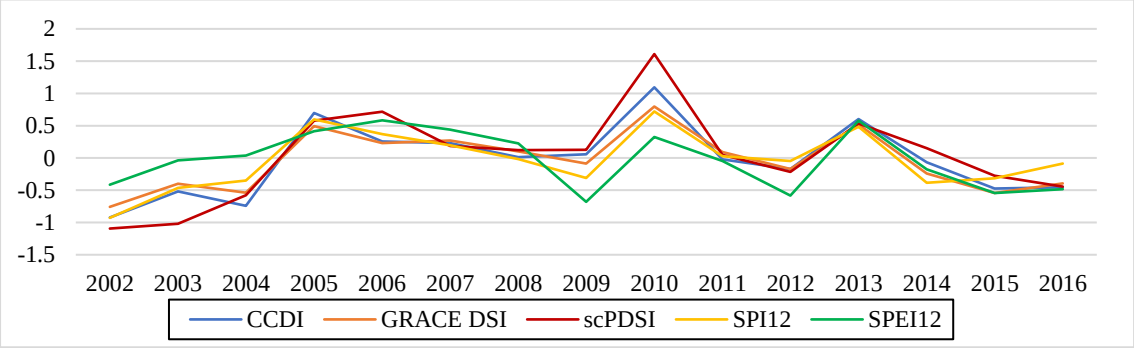

(c) Post monsoon Rabi season

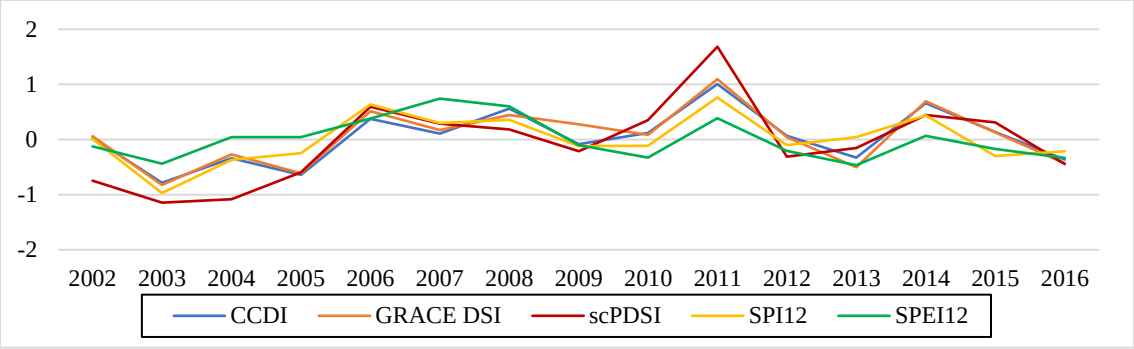

(d) Premonsoon Season

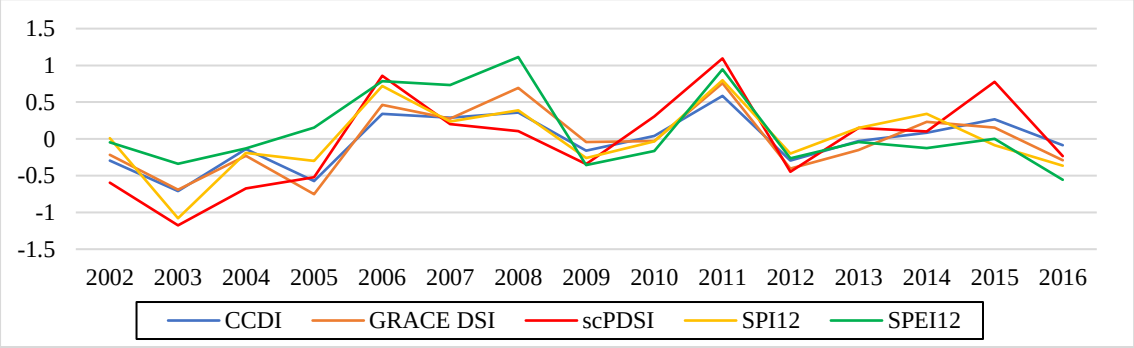

Figure 3

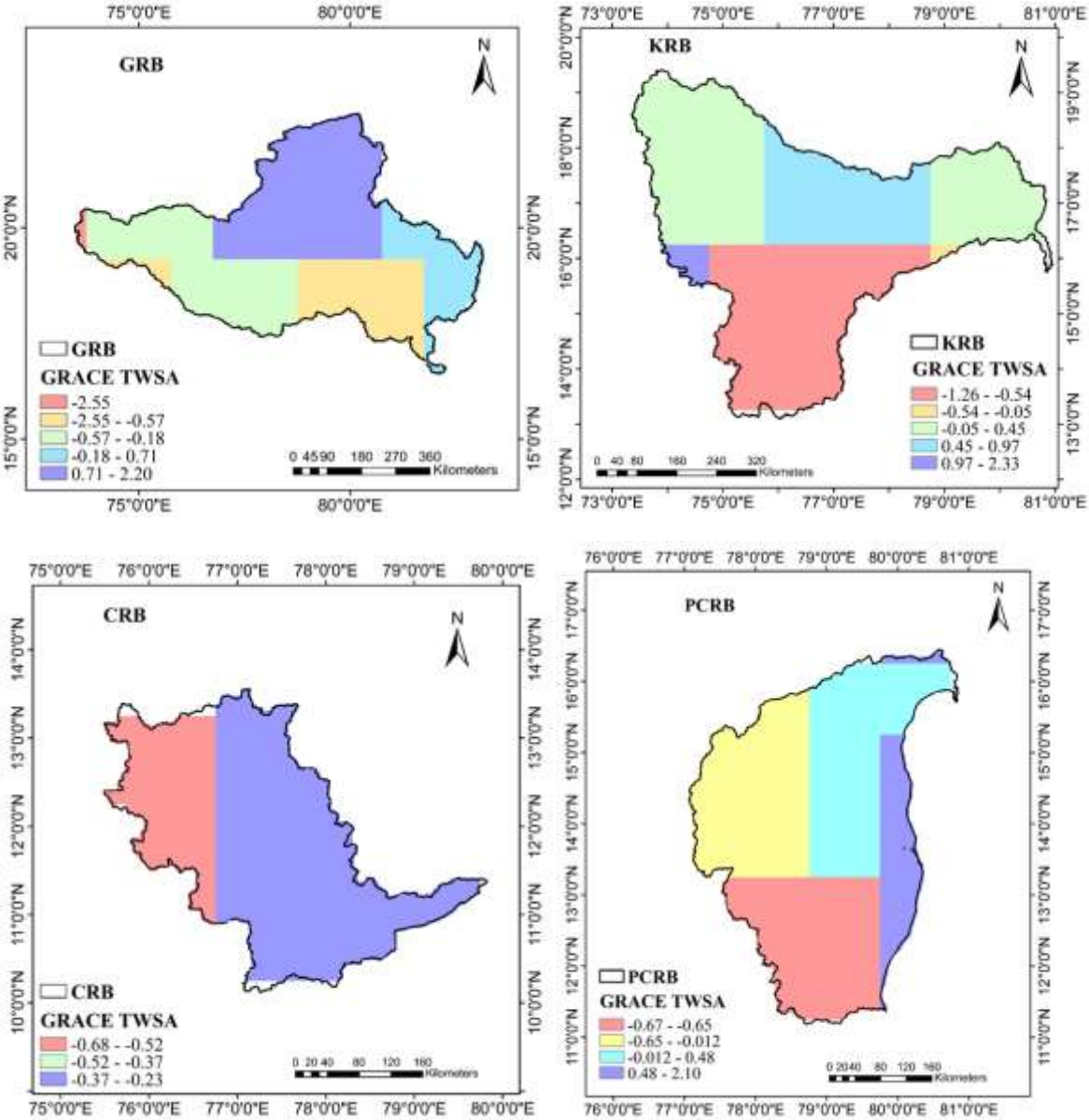
GRB
GRB
GRACE TWSA
-2.55
-2.55 - -0.57
-0.57 - -0.18
-0.18 - 0.71
0.71 - 2.20
Kilometers
KRB
KRB
GRACE TWSA
-1.26 - -0.54
-0.54 - -0.05
-0.05 - 0.45
0.45 - 0.97
0.97 - 2.33
Kilometers
CRB
CRB
GRACE TWSA
-0.68 - -0.52
-0.52 - -0.37
-0.37 - -0.23
Kilometers
PCRB
PCRB
GRACE TWSA
-0.67 - -0.65
-0.65 - -0.012
-0.012 - 0.48
0.48 - 2.10
Kilometers

Figure 4

(a) GRB

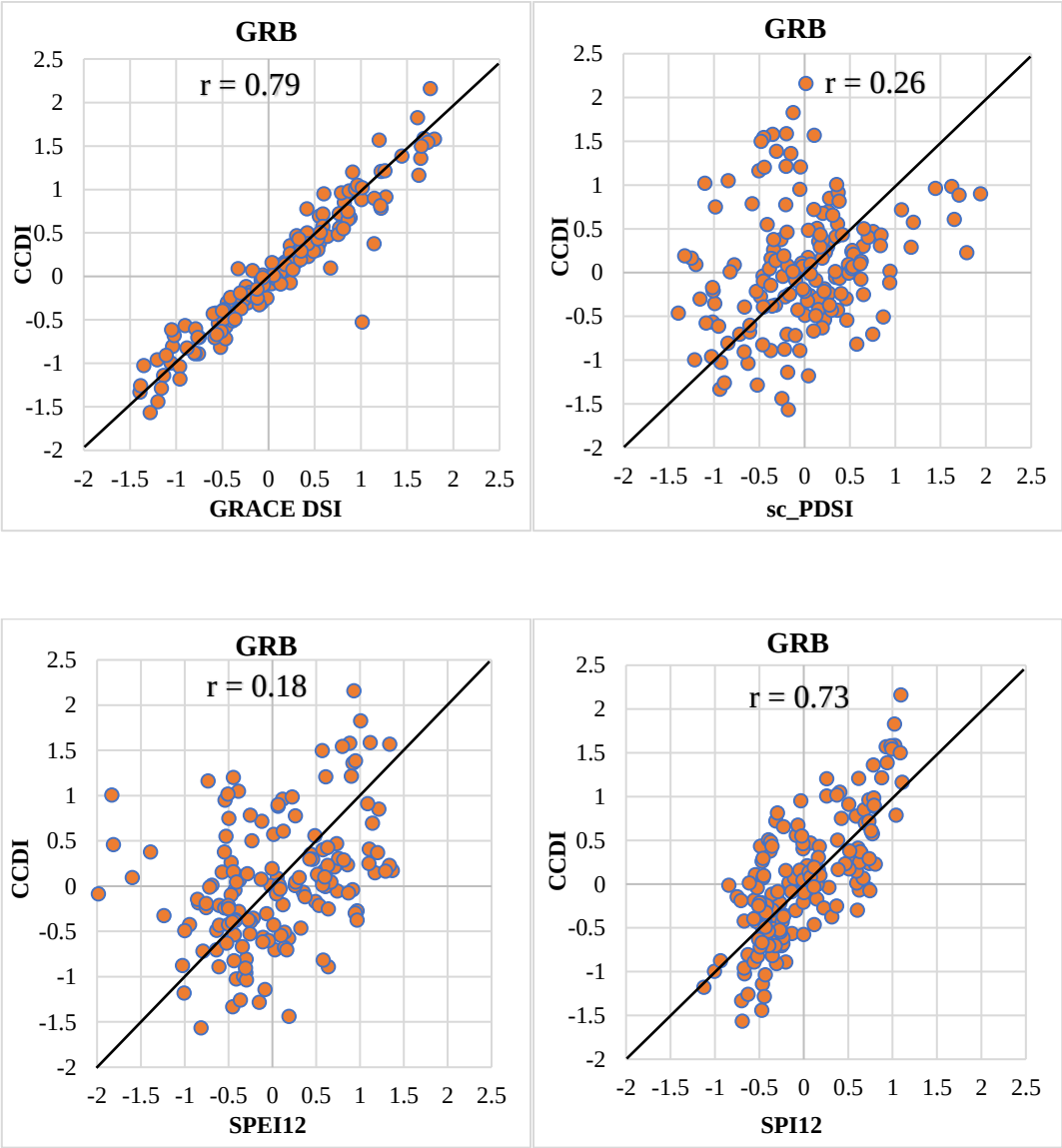
GRB
r = 0.79
CCDI
GRACE DSI
GRB
r = 0.26
CCDI
sc_PDSI
GRB
r = 0.18
CCDI
SPEI12
GRB
r = 0.73
CCDI
SPI12

(b) KRB

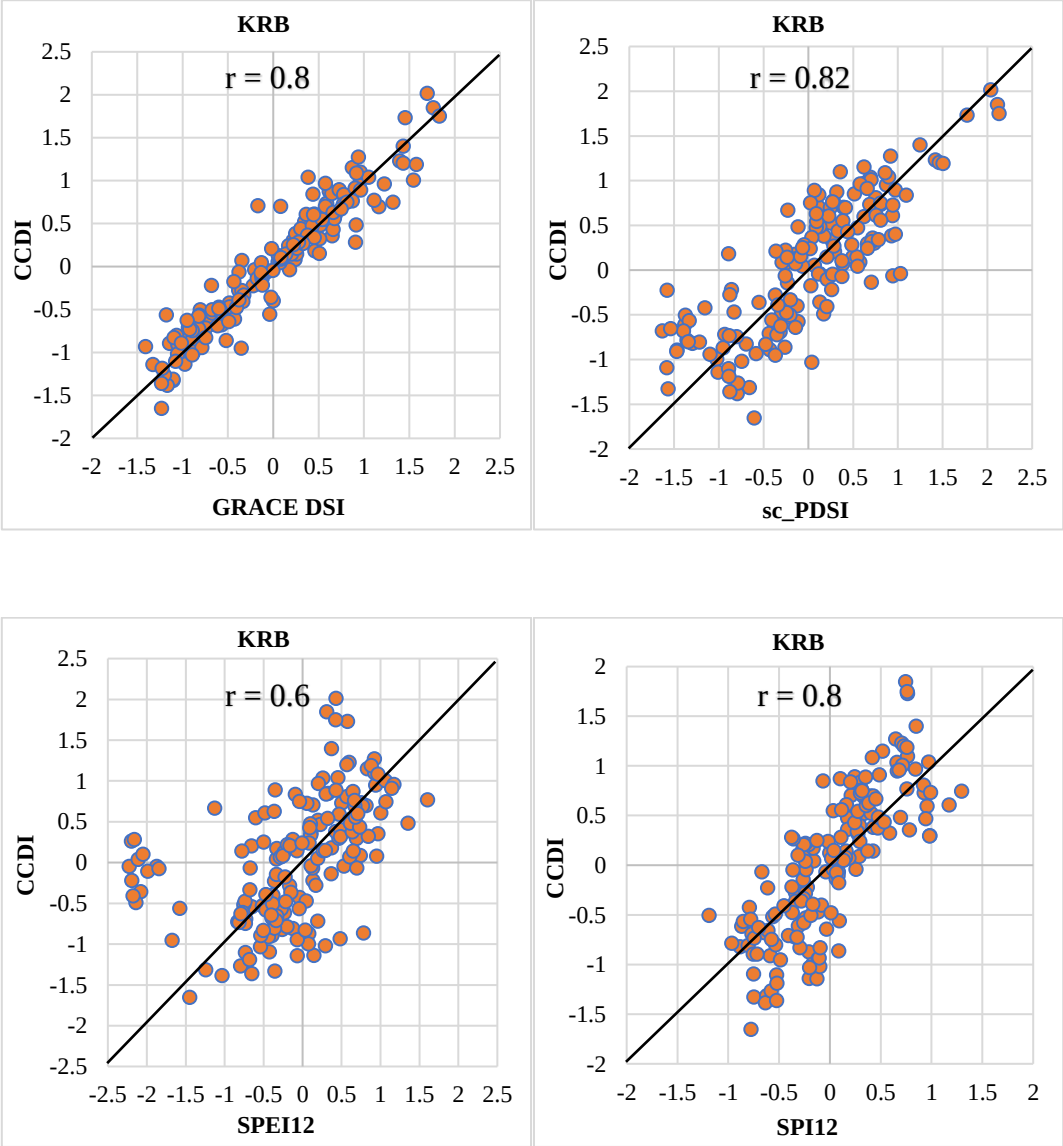
KRB
r = 0.8
CCDI
GRACE DSI
KRB
r = 0.82
CCDI
sc_PDSI
KRB
r = 0.6
CCDI
SPEI12
KRB
r = 0.8
CCDI
SPI12

(c) CRB

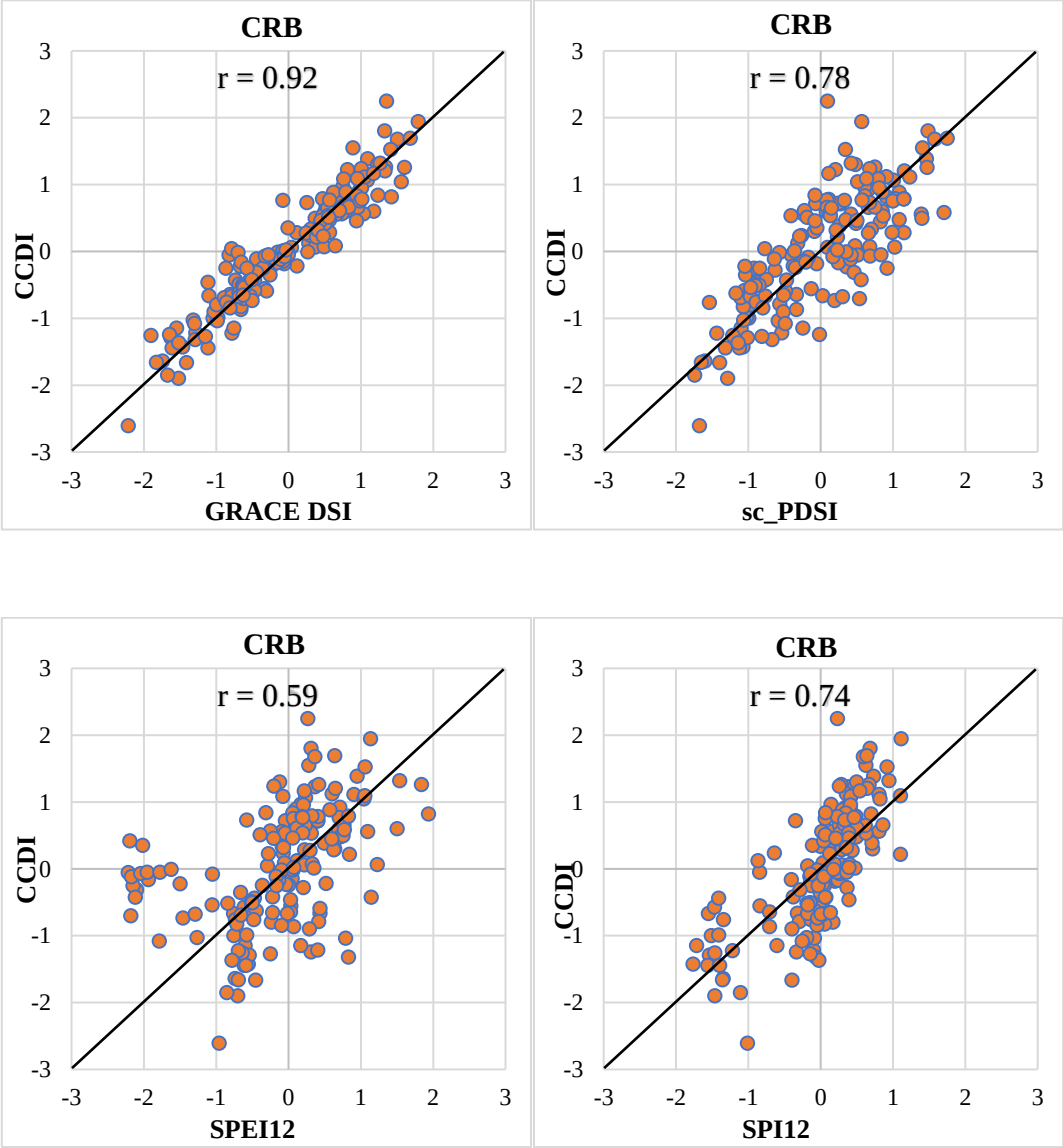
CRB
r = 0.92
CCDI
GRACE DSI
CRB
r = 0.78
CCDI
sc_PDSI
CRB
r = 0.59
CCDI
SPEI12
CRB
r = 0.74
CCDI
SPI12

(d) PCRB

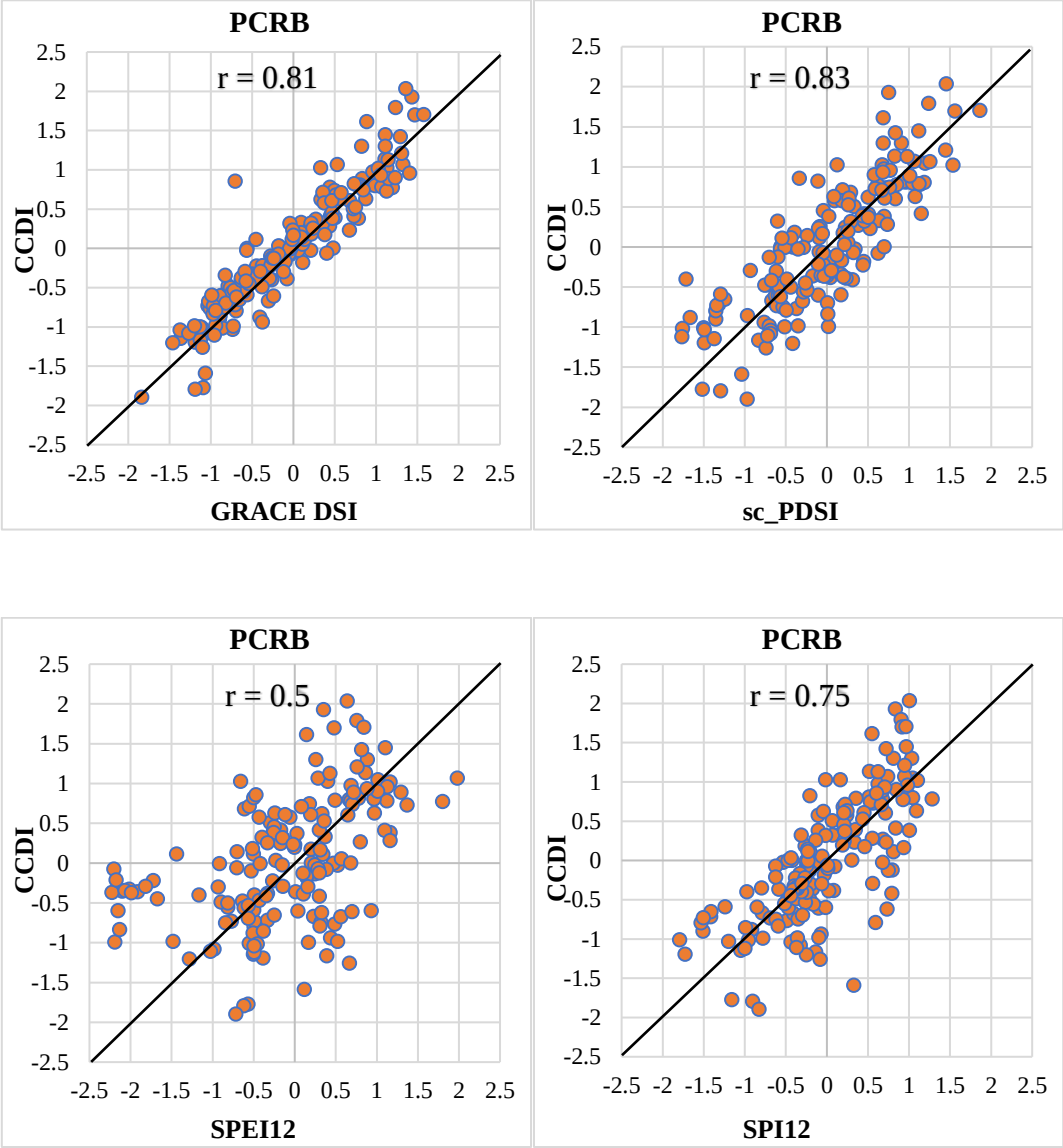

Figure 5

(a)

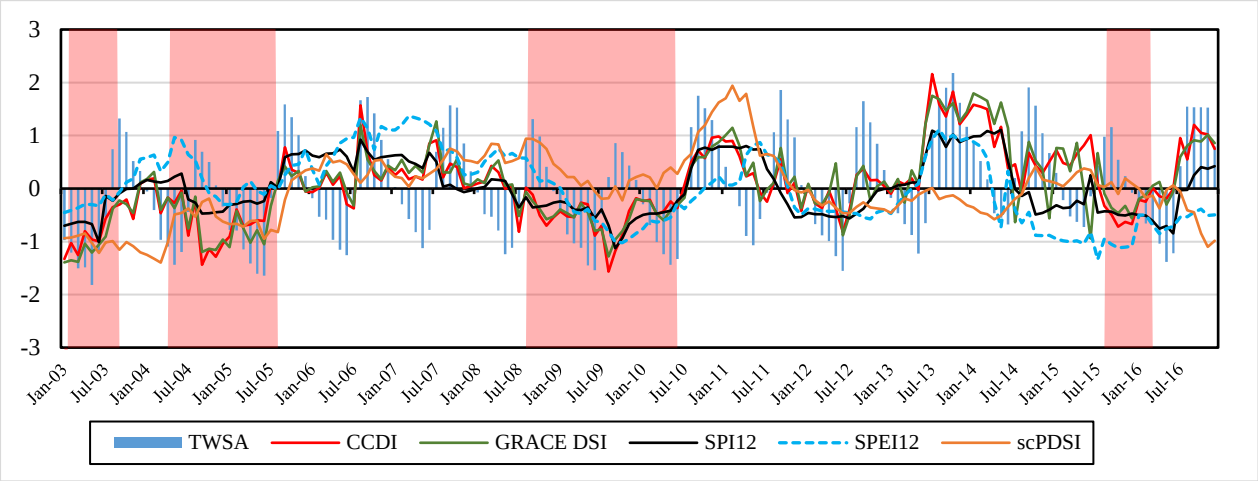
3
2
1
0
-1
-2
-3
Jan-03
Jul-03
Jan-04
Jul-04
Jan-05
Jul-05
Jan-06
Jul-06
Jan-07
Jul-07
Jan-08
Jul-08
Jan-09
Jul-09
Jan-10
Jul-10
Jan-11
Jul-11
Jan-12
Jul-12
Jan-13
Jul-13
Jan-14
Jul-14
Jan-15
Jul-15
Jan-16
Jul-16
TWSA
CCDI
GRACE DSI
SPI12
SPEI12
scPDSI

(b)

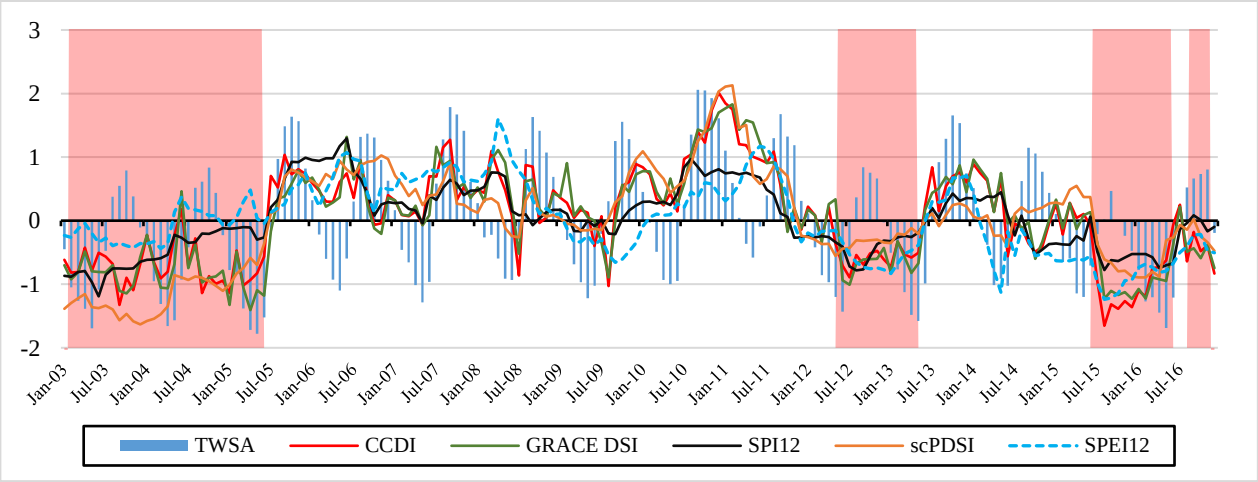
3
2
1
0
-1
-2
Jan-03
Jul-03
Jan-04
Jul-04
Jan-05
Jul-05
Jan-06
Jul-06
Jan-07
Jul-07
Jan-08
Jul-08
Jan-09
Jul-09
Jan-10
Jul-10
Jan-11
Jul-11
Jan-12
Jul-12
Jan-13
Jul-13
Jan-14
Jul-14
Jan-15
Jul-15
Jan-16
Jul-16
TWSA
CCDI
GRACE DSI
SPI12
scPDSI
SPEI12

(c)

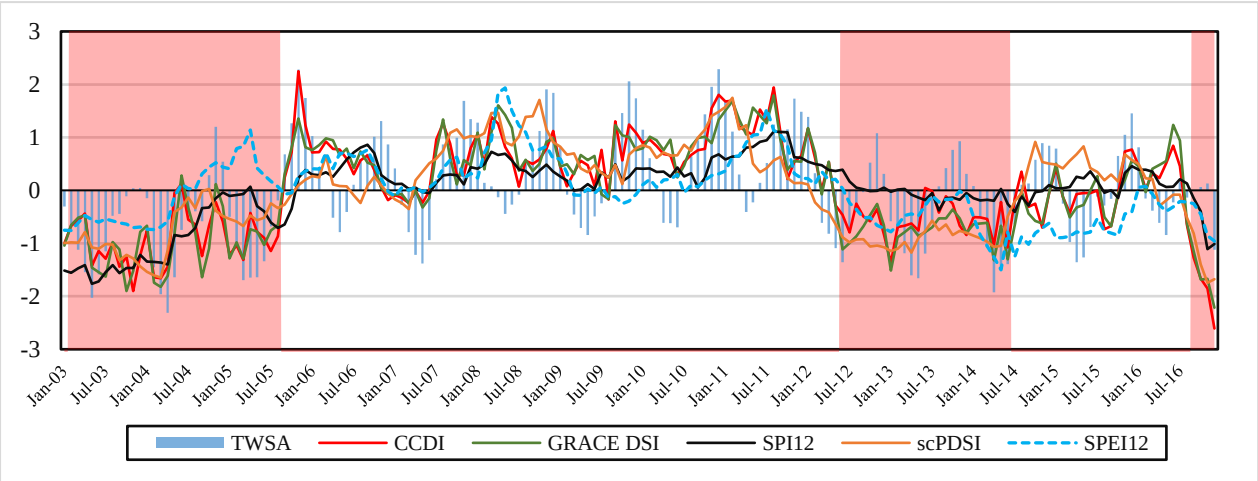
3
2
1
0
-1
-2
-3
Jan-03
Jul-03
Jan-04
Jul-04
Jan-05
Jul-05
Jan-06
Jul-06
Jan-07
Jul-07
Jan-08
Jul-08
Jan-09
Jul-09
Jan-10
Jul-10
Jan-11
Jul-11
Jan-12
Jul-12
Jan-13
Jul-13
Jan-14
Jul-14
Jan-15
Jul-15
Jan-16
Jul-16
TWSA
CCDI
GRACE DSI
SPI12
scPDSI
SPEI12

(d)

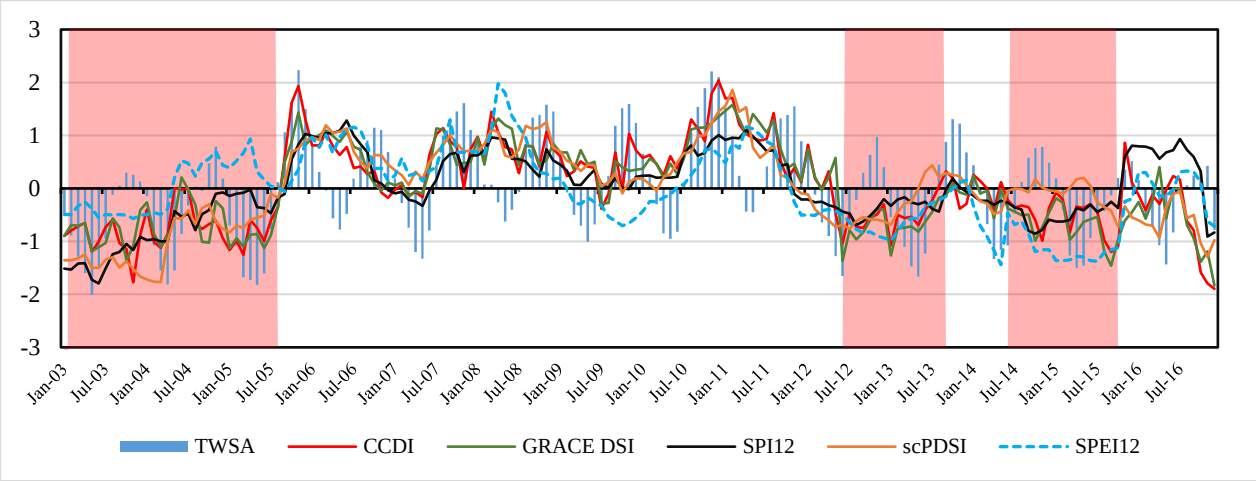

Figure 6

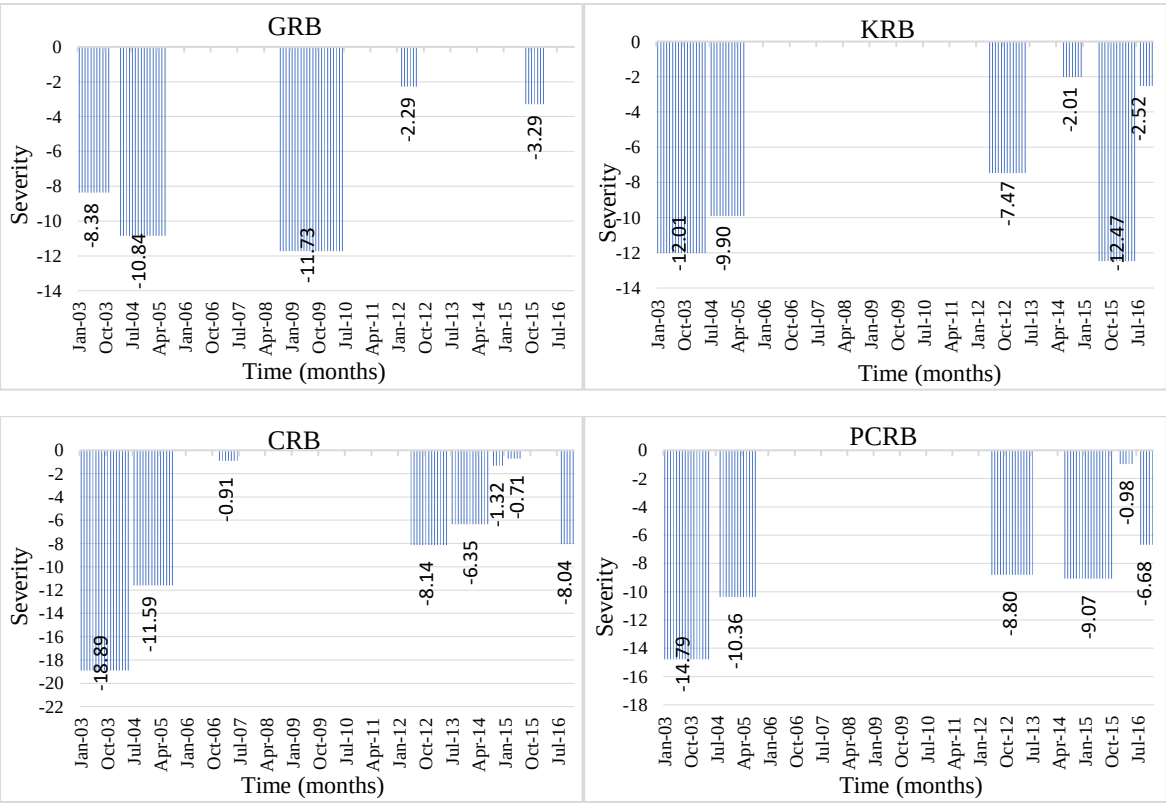

Figure 7

971

List of Tables

Table 1 River basin details considered for the study

Table 2 (a) Drought categories related to dry (D) conditions for SPI

Table 2 (b) Drought categories related to wet (W) and dry (D) conditions for GRACE DSI and CCDI

Table 3 Correlation of TWSA with short and long reference periods of SPI 3, 6, and 12

Table 4 Correlation matrix of drought indices computed for four river basins in India.

Table 5 Statistical metrics between GRACE TWSA and drought indices (CCDI, GRACE DSI, scPDSI, SPEI12, and SPI12) computed for four river basins in India.

Table 6 Summary of drought severity and duration calculated from CCDI for the drought events identified over four river basins in India.

Table 1 River basin details considered for the study

S. No	Basin Name	Area (Sq.km)	Mean Annual Rainfall (mm)	Maximum Temperature (°C)	Minimum Temperature (°C)	Elevation (m)
1	Godavari (GRB)	3,12,812	1093.21	33.04	20.63	1664
2	Krishna (KRB)	2,54,750	859.11	32.14	20.52	1903
3	Pennar and East flowing rivers between Pennar and Cauvery (PCRB)	1,17,889	770.18	32.71	21.63	1439
4	Cauvery (CRB)	85,626	1075.23	34.31	17.15	2629

Table 2(a) Drought categories related to dry (D) conditions for SPI (McKee et al., (1993))

Drought Category	SPI
D0: Mild (abnormal) Drought	0 to -0.99
D1: Moderate Drought	-1.00 to -1.49
D2: Severe Drought	-1.50 to -1.99
D3: Extreme Drought	≤ 2

Table 2(b) Drought categories related to wet (W) and dry (D) conditions for GRACE DSI and CCDI (Zhao et al. (2017a))

Drought Category	GRACE DSI and CCDI
W4: Exceptionally Wet	2 or greater
W3: Extremely Wet	1.6 to 1.99
W2: Severely Wet	1.3 to 1.59
W1: Moderately Wet	0.8 to 1.29
W0: Abnormally Wet	0.5 to 0.79
N: Near Normal	0.49 to -0.49
D0: Abnormally Dry	-0.5 to -0.79
D1: Moderately Dry	-0.8 to -1.29
D2: Severely Dry	-1.3 to -1.59
D3: Extremely Dry	-1.6 to -1.99
D4: Exceptionally Dry	-2 or less

Table 3 Correlation of TWSA with short and long reference periods of SPI 3, 6, and 12

	L-SPI3	**L-SPI6**	**L-SPI12**	**S-SPI3**	**S-SPI6**	**S-SPI12**
GRB-TWSA	0.21	0.24	0.32	0.19	0.25	0.36
KRB-TWSA	0.2	0.26	0.4	0.23	0.31	0.37
CRB-TWSA	0.27	0.35	0.48	0.3	0.36	0.43
PCRB-TWSA	0.24	0.31	0.4	0.19	0.33	0.42

Table 4 Correlation matrix of drought indices computed for four river basins in India.

	CCDI	GRACE DSI	sc_PDSI	SPEI12	SPI12
Godavari					
CCDI	1				
GRACE DSI	0.79	1			
sc_PDSI	0.26	0.22	1		
SPEI12	0.18	0.17	0.15	1	
SPI12	0.73	0.59	0.30	0.78	1
Krishna					
CCDI	1				
GRACE DSI	0.80	1			
sc_PDSI	0.82	0.67	1		
SPEI12	0.60	0.52	0.53	1	
SPI12	0.80	0.66	0.78	0.75	1
Cauvery					
CCDI	1				
GRACE DSI	0.92	1			
sc_PDSI	0.78	0.75	1		
SPEI12	0.59	0.59	0.68	1	
SPI12	0.74	0.67	0.68	0.71	1
Pennar					
CCDI	1				
GRACE DSI	0.81	1			
sc_PDSI	0.83	0.70	1		
SPEI12	0.50	0.51	0.65	1	
SPI12	0.75	0.61	0.77	0.74	1

Table 5 Statistical metrics between GRACE TWSA and drought indices (CCDI, GRACE DSI, scPDSI, SPEI12, and SPI12) computed for four river basins in India.

Godavari (GRB)				
		R^2	**RMSE**	**MSE**
CCDI	GRACE DSI	0.81	0.22	0.04
	sc_PDSI	0.19	0.81	0.66
	SPEI12	0.15	0.92	0.87
	SPI12	0.54	0.46	0.21
Krishna (KRB)				
CCDI	GRACE DSI	0.89	0.26	0.05
	sc_PDSI	0.68	0.40	0.2
	SPEI12	0.24	0.78	0.62
	SPI12	0.64	0.45	0.2
Pennar and East flowing rivers between Pennar and Cauvery (PCRB)				
CCDI	GRACE DSI	0.87	0.24	0.06
	sc_PDSI	0.69	0.41	0.24
	SPEI12	0.21	0.83	0.7
	SPI12	0.56	0.52	0.23
Cauvery (CRB)				
CCDI	GRACE DSI	0.9	0.27	0.07
	sc_PDSI	0.62	0.55	0.3
	SPEI12	0.21	0.89	0.79
	SPI12	0.55	0.51	0.34

Table 6 Summary of drought severity and duration calculated from CCDI for the drought events identified over four river basins in India.

Time period	Severity	Duration (No. of months)
Godavari (GRB)		
Jan to Nov 2003	-8.37555	11
Mar 2004 to Jun 2005	-10.842	16
Sep 2008 to Jun 2010	-11.7261	22
Feb to Jul 2012	-2.29115	6
Aug 2015 to Feb 2016	-3.29387	7
Krishna (KRB)		
Jan 2003 to May 2004	-12.0102	17
Jul 2004 to Jun 2005	-9.90192	12
May 2012 to May 2013	-7.46998	13
Jun to Dec 2014	-2.00988	7
Jul 2015 to Jun 2016	-12.466	13
Aug to Dec 2016	-2.51763	5
Pennar and East flowing rivers between Pennar and Cauvery (PCRB)		
Jan 2003 to Apr 2004	-14.7907	16
Aug 2004 to Aug 2005	-10.3604	13
May 2012 to Jul 2013	-8.7965	15
Jun 2014 to Oct 2015	-9.07017	17
Jan to May 2016	-0.978	5
Aug to Dec 2016	-6.68397	5
Cauvery (CRB)		
Jan 2003 to May 2004	-18.8912	17
Jul 2004 to Aug 2005	-11.5941	14
Dec 2006 to Jun 2007	-0.91175	7
May 2012 to May 2013	-8.14022	13
Jul 2013 to Jul 2014	-6.34736	13
Sep to Dec 2014	-1.32244	4
Feb to Jun 2015	-0.7066	5
Aug to Dec 2016	-8.04247	5